Article

https://doi.org/10.1007/s12303-023-0027-4
pISSN 1226-4806 eISSN 1598-7477

Geosciences Journal GJ

# Geochemistry and geochronology of Middle Eocene subduction-related felsic volcanics in the Misis-Andirin Complex of the Southeast Anatolian Orogenic Belt

Nusret Nurlu[1]*, Ahmet Can Akinci[1], and Milan Kohút[2]

[1]Department of Geological Engineering, Faculty of Engineering, Cukurova University, 01330 Balcali-Adana, Turkey
[2]Earth Science Institute, Slovak Academy of Sciences, 840 05 Bratislava, Slovakia

**ABSTRACT:** LA-ICP-MS zircon geochronology and geochemistry (whole-rock & mineral chemistry) from the Misis-Andirin Complex (MAC) volcanic rocks are reported. The MAC records magmatic, sedimentary, and tectonic processes operating at the northern active margin of the Neotethys (South Tethys) in the eastern Mediterranean district. The MAC represents an association of an originally active continental margin including the Engizek (in the NE), Andirin (central) and Misis (in the SW) segments. The felsic extrusives are depleted in HFSE (high-field-strength elements), enriched in LILE (large-ion lithophile elements) and have flat-type REE patterns; these trends and also biotite chemistry verify their supra-subduction zone tectonic environment. The studied volcanic unit consists of mainly rhyolite, dacite and rare andesite rocks, and is intercalated with Bulgurkaya Formation. These felsic extrusive rocks show relative depletions in Ti + Nb, and partial enrichment in Cs, Rb, Ba, and Th in the N-MORB (normal-mid ocean ridge basalt) normalized spider plot, suggesting their derivation from a supra-subduction geodynamic environment. The La/Nb (1.92–2.33) and Nb/Th (1.0–1.12) ratios of all the analysed extrusives from Andirin region present arc magmas or volcanic rocks affinity that could have been contributed by crustal source contents and also examined volcanics yield nearly flat Ba/La ratios with relatively increasing Th/Yb, suggesting the contribution of sediments or crustal contamination. The Al-in-hornblende thermobarometry (2.04 to 1.55 kbar) of Mg-Fe hornblende in the volcanics of the MAC represents their crystallization of amphibole in the moderate to shallow crustal level at a maximum 6.7 km to a minimum 5.1 km depth. The ilmenite-magnetite thermometer based on Fe-Ti oxide equilibria shows that the Andirin region felsic magmas were at 717 ℃ and at an $fO_2$ of approximately 2.16 log units (+1.51 NNO). The MAC extrusive volcanic rocks were produced throughout the Eocene period, and our new U-Pb zircon dating (47.13 ± 0.5 Ma) confirmed mainly younger Lutetian age of the volcanic activity in the Andirin area.

**Key words:** felsic volcanics, Misis-Andirin Complex, SE Anatolia, island arc, U-Pb zircon

Manuscript received February 23, 2023; Manuscript accepted June 4, 2023

## 1. INTRODUCTION

One of the most complicated parts of the Alpine-Himalayan system is the Misis-Andirin Complex (MAC), located among the Tauride/Anatolide Platform and the Arabian Platform. Sutured relicts of the South Neotethys are extended through the south-eastern Anatolia into Iran (Şengör and Yılmaz, 1981; Robertson et al., 1991; Yılmaz, 1993; Robertson, 2004) and the Misis-Andirin Complex (MAC), located among the Tauride/Anatolide Platform and the Arabian Platform (Fig. 1). It is broadly accepted that South Neotethys was gradually closed throughout the Late Cretaceous–Miocene time interval in reaction to subduction, collisional and strike-slip processes (Hall, 1976; Aktaş and Robertson, 1984; Yılmaz, 1993; Robertson et al., 2006; Furman et al., 2021; Gall et al., 2021). However, the Late Cretaceous to Miocene geodynamics of the region's objective tectonic scenario is important for identification of the time evolution along the southeast Anatolian Orogenic Belt and also the MAC. After passing through the Misis Mountains, the

Editorial responsibility: Sung Hi Choi

***Corresponding author:**
Nusret Nurlu
Department of Geological Engineering, Faculty of Engineering, Cukurova University, 01330 Balcali-Adana, Turkey
Tel: +90-322-333386715, E-mail: nusretnurlu@gmail.com

**Electronic supplementary material**
The online version of this article (https://doi.org/10.1007/s12303-023-0027-4) contains supplementary material, which is available to authorized users.

©The Association of Korean Geoscience Societies and Springer 2023

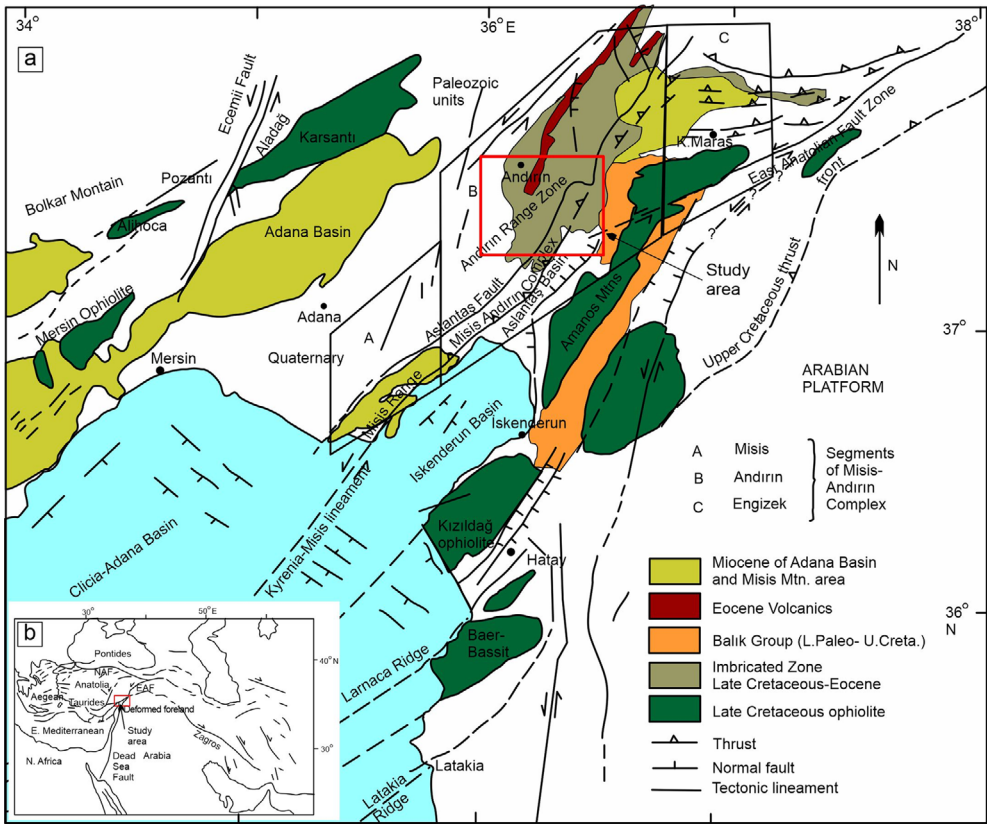



**Fig. 1.** (a) Tectonic map of the Anatolia and surroundings presenting the location of the study area (red square) (Robertson, 2004). (b) The geodynamic map of the MAC and surroundings presents mainly three segments; Engizek (east), Andirin (middle) and Misis (west) evaluated in this research (colourised after Robertson, 2004).

Misis-Andirin lineation continues under the Mediterranean Sea in the southwest direction and continues until the Kyrenia range, where similar lithologies were exposed (Robertson, 2004). The mechanism and timing of collision and subduction of the Arabian (North Africa) against Anatolian (Eurasian) plates are controversial issues yet. The suture connecting the Eastern Mediterranean basin with south-eastern Anatolia lies down through the Engizek, Andirin, and Misis Mountains chain of the South Anatolia (Fig. 1).

The studied felsic volcanic rocks are well exposed in the Andirin region along with the Misis-Andirin Complex, Kahramanmaraş area of the S Turkey (Figs. 2 and 3); though their crystallisation age, geodynamic significance and origin are poorly documented. In the Andirin region the volcanic rocks were mentioned for the first time by Yılmaz and Gürer (1996). Nevertheless, no data other than petrography and tectonomagmatic stratigraphic relations of the unit were presented. The felsic volcanic rocks observed in the Misis (Ceyhan, Adana) region and located on the same belt were reported to be of island arc volcanism and their age was revealed as Late Cretaceous by Floyd et al. (1991). Located in the central part of the Alpine-Himalayan belt, the Anatolian peninsula consists of several platforms, having origin in the Tethyan Ocean, which were tectonically uplifted from the Late Cretaceous and has become a high plateau. Especially, the east-west trending oceanic crust fragments belonging to the Neotethys formed ophiolitic belts and then have subducted under these platforms and formed several ophiolitic belts during the period from Late Cretaceous to Miocene. Along these subduction zones, several mélange units have also been formed together with the ophiolite emplacement (Hall, 1976; Şengör and Yılmaz, 1981; Aktaş and Robertson, 1984; Robertson and Dixon, 1984; Dewey et al., 1986; Robertson et al., 1991; Yılmaz, 1993; Yılmaz et al., 1993; Stampfli, 2001; Barrier and Vrielynck, 2008; Akıncı et al., 2016; Nurlu, 2016; Nurlu et al., 2016; Akıncı and Ünlügenç, 2021). In this scheme, sediments deposited in related basins that getting narrower with gradual subduction were significantly affected by these compressional tectonic conditions. Although most of the studies carried out in the region suggest that the basins were mostly closed and collisional processes started in the Miocene period, especially in the south and south-eastern Anatolia, the details of these processes have still not been revealed clearly. The aim of our study is to bring missing data needed for solving the evolution puzzle of the MAC. This research reports new geochronological

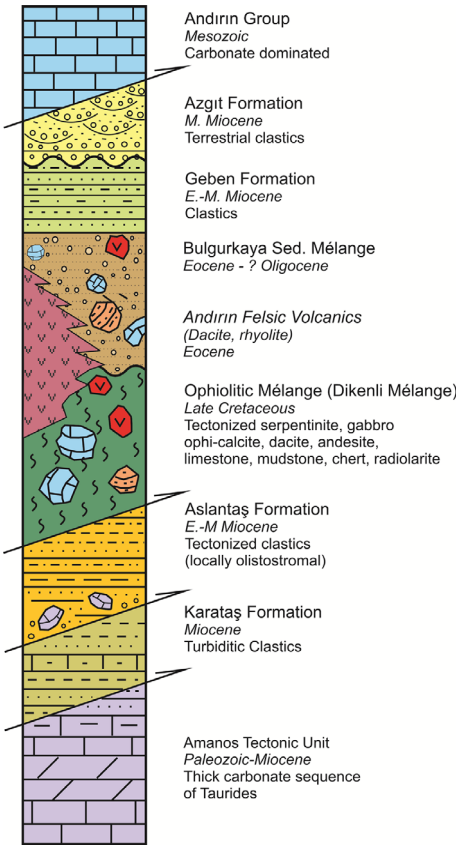



**Fig. 2.** Columnar section showing tectonostratigraphic relations of the units observed in the Andirin region (modified from Akıncı and Ünlügenç, 2021).

(LA-ICP-MS U-Pb zircon), geochemical (whole-rock & mineral chemistry) and detail petrographic data in an attempt to shed light on the tectonic setting of the Andirin felsic volcanics and/or general the Eocene–Miocene tectonomagmatic evolution of the MAC owing to old and new information. In the light of these data, the geodynamic environment of this unit will be revealed and it will be compared with the volcanics of similar age and geochemical characteristics in the Southeastern Anatolian Orogenic Belt (SAOB).

## 2. GEOLOGICAL SETTING

The basement of the tectonostratigraphic sequence, in the studied Andirin region (Kahramanmaraş – SE Anatolia), is made up of sedimentary sequence of the Amanos Group, which generally represents the north-western margin of the subducted Arabian platform. The Amanos Group is a thick sequence dominated by carbonate rocks deposited from Mesozoic to Miocene (Yalçin, 1980; Usta et al., 2015; Duman et al., 2017). Whereas the Karataş and Aslantaş Formations – the Early–Middle Miocene in age, were deposited in the thrust front basin, and generally lie on top of the sequence, often with tectonic contact. On this slice, there are a mélange unit (Bulgurkaya and Dikenli Fm.) that are underlain the Tauride platform by tectonic contact and sedimentary cover units deposited on them (Figs. 3 and 4). At the base of this series is the Late Cretaceous Dikenli Mélange, which is in the nature of an ophiolite-related mélange, and the Bulgurkaya Formation, which show a sedimentary mélange character (Akıncı et al., 2015; Akıncı and Ünlügenç, 2021). These two units together are equivalent to the Misis Mélange of many authors along the Misis Range (e.g., Gökçen et al., 1988; Robertson, 2004). The Eocene–Oligocene age Bulgurkaya Formation is including intermediate volcanic rocks and is conformably overlain by the Early Middle Miocene Geben Formation. Exposed at the top of this cover sequence, coming on a low degree of angular unconformity the Azgıt Formation represented by Middle Miocene aged terrestrial clastics. All these units in the Suture zone are tectonically overlain by nappes of Mesozoic Andirin Group carbonate rocks belonging to the Tauride platform together with the cover units.

### 2.1. Amanos Group

The Amanos Group represents the Arabian Foreland units in the south of the imbrication zone in the Andirin region and the unit includes the Mesozoic Balk Group (dominated by Mesozoic neritic carbonates) and the Miocene Kalecik (dominated by coarse grained terrestrial clastics), the Horu (reef carbonates) and the Kızıldere Formations. The Kızıldere Formation, located on the Horu Formation, forms the upper part of the Amanos Group and represented mainly by sandstone, mudstone and marl alternations (Yılmaz and Gürer, 1996; Ikram and Varol, 2011).

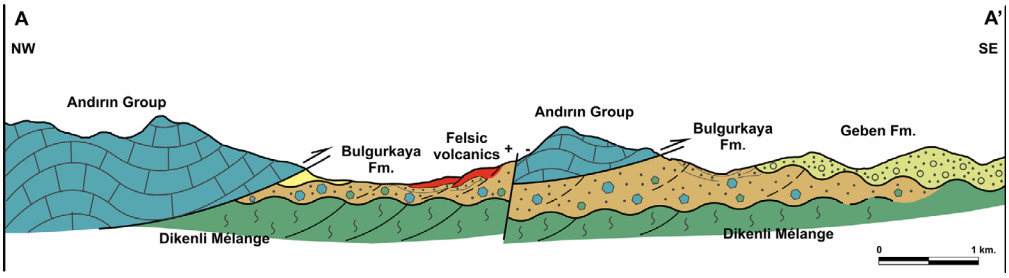



**Fig. 3.** A cross-section presenting the field relations of the Andirin region of MAC.


https://doi.org/10.1007/s12303-023-0027-4

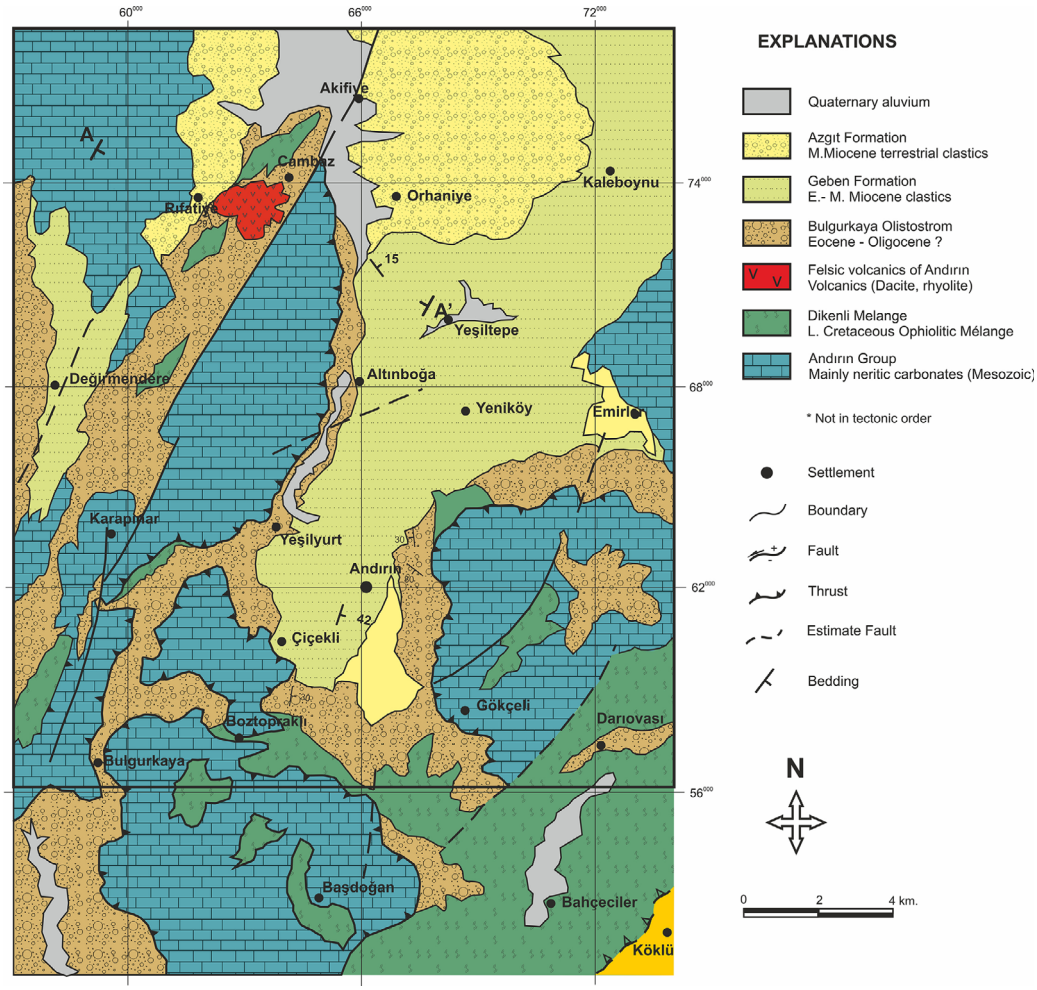



**Fig. 4.** Geological map of the Andirin region including the studied felsic volcanic rocks (modified after Akıncı and Ünlügenç, 2021).

## 2.2. Imbrication Zone

In the southern parts of the study area, the Karataş and Aslantaş Formations, which give outcrops along the imbrication zone (Robertson, 2004) (Karatepe Thrust – SE of the study area), were tectonically overlain by the mélange units (Dikenli Formation) in the northeast and underlain the Amanos Group. The Aslantaş Formation has a turbiditic sequence character and consists of alternation of sandstone, shale and marl. The sequence is highly deformed and contains olistoliths in places. For the age of the unit, Kozlu (1987) proposed the Lower Langhian–Serravallian range based on the nannoplankton content. Tectonically underlying the Aslantaş Formation is the Karataş Formation, which is also a turbiditic unit. The Karataş Formation, which is dominated by alternation of sandstone and shale, is less deformed than Aslantaş Formation and offers a more regular sequence character. The Tb-Te layers of the Bouma turbidite sequence can be observed within the unit (Yılmaz and Gürer, 1996). Kelling et al. (1987) proposed the Burdigalian–Tortonian age range for the unit in the study he conducted on the outcrops around the Karataş district of Adana (Mediterranean coast), which is the type locality of the unit.

## 2.3. Ophiolitic/Sedimentary Complexes on the Tauride Belt

The Upper Cretaceous Mélange, which presents an ophiolitic mélange at the bottom, is located in the imbrication zone in the study area. The unit is tectonically overly the Aslantaş Formation in the south and is overlain by the Bulgurkaya Formation with a tectonic contact locally. The Dikenli Mélange generally consists of tectonized serpentinites, basic volcanics, andesite, shale and olistostromal clastics. Although the internal structures of the unit are generally tectonized and not well exposed, there are also levels of debris flow product containing carbonate blocks derived from the Andirin Group nappe. The Bulgurkaya Formation, which presents less deformed features, shows olistostromal blocks character, is located on the Dikenli Mélange (Figs. 2 and 3).

Because the boundary between these two units is tectonically deformed and does not present a sharp transition therefore the

boundary is not clear due to the complex nature of the both units. The Bulgurkaya Formation gives outcrops in and around the Bulgurkaya village, where it has type section. The blocks of the unit, which presents a sedimentary mélange feature, are generally derived from carbonates of the Andirin Group and occasionally from the Dikenli Formation. The matrix of the unit is generally the debris flows similar to these blocks and other fine-grained clastics deposited in the basin. Age ranges ranging from the Early Eocene to Early Miocene have been proposed for the Bulgurkaya Formation (Yılmaz and Gürer, 1996; Kozlu, 1997; Robertson, 2004).

### 2.4. Andirin Group

The unit, which generally presents the characteristic a thick carbonate sequence of Mesozoic age in the study area, is called Andirin Group within the Taurus Tectonic Group (Ayaşlıoğlu, 1970). These rocks are exposed along the Misis-Andirin range, generally on ophiolitic or volcaniclastic complexes and occasionally as nappes on the Neogene deposits. In addition, these complex units are mostly settled as olistolite blocks in the mélange units and they can reach tens of meters in size. Generally, these high-energy platform carbonates, are mostly neritic and are partly dolomitized. Their outcrops present a very steep and karst morphology. The rocks of the Andirin group are highly tectonized and contain irregularly developed imbrications and fold structures.

### 2.5. Miocene Basinal Cover Units

The Middle Miocene Geben Formation deposited concordantly on the Bulgurkaya Formation in the Andirin region and consists of conglomerate, sandstone, mudstone and marls. The unit contains conglomeratic and olistostromal lenses and pockets in lower levels close to the Bulgurkaya Formation. The Azgıt Formation is the youngest rock unit of the Andirin region, and the unit is located unconformably on the Geben Formation and the Andirin Group. The Azgıt Formation generally consists of sandstone and conglomerates, and also includes limestone and marl levels. The age of the unit is given as Middle Miocene by Yılmaz and Gürer (1996), and as Langhian by Kozlu (1987), based on its fossil content.

## 3. FIELD CHARACTERISTICS OF THE ANDIRIN REGION VOLCANICS

In the northwest part of the study area, volcanic rocks with rhyolite and dacite composition are observed outcropping in the Güzelbeyli (north of Andirin region) region and its immediate surroundings (Figs. 2 and 3). The maximum thickness of the volcanic rocks, which form the basis of the research subject, is approximately 150 meters and these volcanics are observed to outcrop in the north-western part of the Ceneviz and Tırıl Mountains, along a narrow belt extending approximately northeast-southwest.

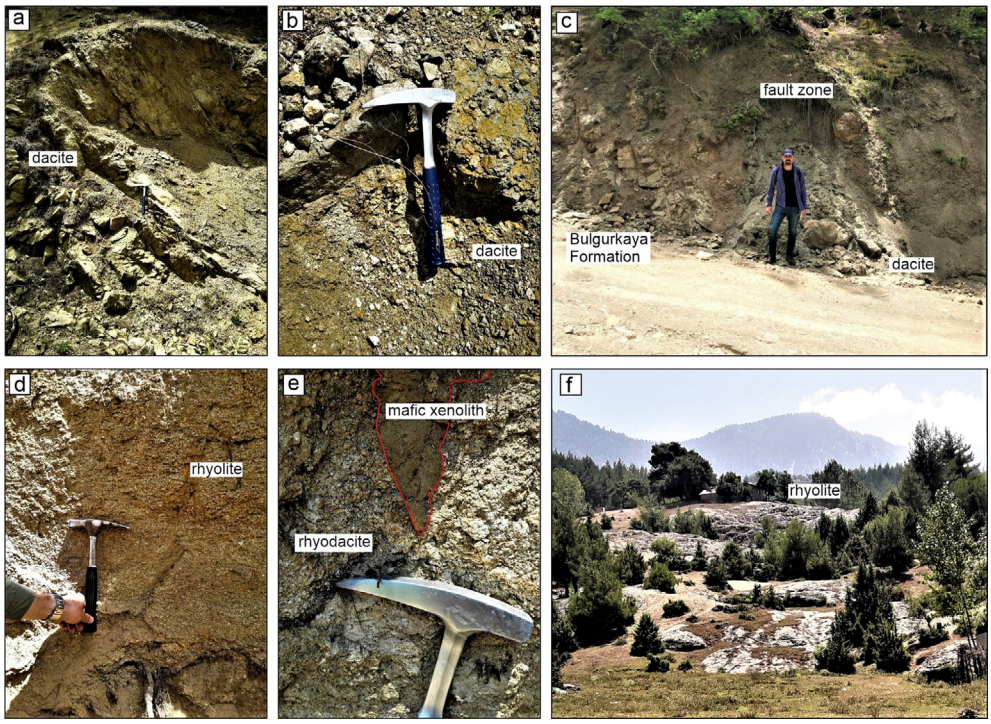



**Fig. 5.** Field occurrences of the felsic volcanics from the MAC. (a and b) general view of dacites belonging to felsic volcanics. (c) Contact relationship between Bulgurkaya Formation and felsic volcanics. (d) Moderately altered rhyolite outcrop. (e) Mafic xenolith observed in rhyodacites. (f) Rhyolitic volcanics of Andirin region.


https://doi.org/10.1007/s12303-023-0027-4

Unaltered surfaces of felsic volcanics, which are represented by flow breccias, lava flows and rarely tuffs, are mostly observed in grey colours (Fig. 5). The studied felsic volcanic rocks, are observed as they has extrusive and locally fault controlled contact with the clastic dominated and bedded upper parts of the Bulgurkaya Formation (northwest of Güzelbeyli village). The primary extrusive contact with the Bulgurkaya Formation probably has subsequently gained a tectonic character as a result of ongoing tectonic compression. These volcanics with varying composition from felsic to basic form outcrop directly on the mélange complex along the Misis Mountains belt (Yılmaz et al., 1985). This tectonic/magmatic position suggests that they were developed either on a directly uplifted accretionary prism or in a submarine environment, but again on a mélange-based succession (Yılmaz and Gürer, 1996). These complex units are locally penetrated by an andesitic volcanism around the Andirin region. The timing and geological setting of this volcanism is the main subject of the study. While the highly deformed marine clastic (turbidite) units of Miocene age are deposited along the suture line in the south-east of the region, the Miocene sediments are exposed in the basin conditions that become shallower to the continental on the ophiolitic and complex units further northwest. The carbonate rocks of Andirin group belonging to the Tauride belt are generally exposed as nappes in the region and also the giant blocks (olistoliths) in the mélange units.

## 4. ANALYTICAL PROCEDURES

### 4.1. Petrographical Analyses

The rhyolitic and dacitic volcanic rock samples were initially studied in thin sections by means of polarization microscopy (ca. 115 thin sections) after field work, what enabled focused secondary rocks sampling suitable for petrological analysis.

### 4.2. Analyses of the Extrusive Rocks

The felsic volcanics sampling was realised from unaltered and fresh outcrops in the study area. A total number of 12 volcanic rocks samples were analysed for major, trace and REE elements. Whole-rock geochemistry of samples AN-1, AN-2, AN-3, AN-9, AN-11, AN-13, AN-12, AN-5, AN-14, AN-7, AN-4, and AN-22 were determined at the ACME Analytical Laboratories Ltd. in Vancouver (Canada). Total abundances of the major oxides were obtained by ICP-OES (Inductively Coupled Plasma Optical Emission Spectroscopy), and trace elements by ICP-MS (Mass Spectroscopy). Sample preparations follow a $LiBO_2$ fusion and dilute nitric digestion for major oxides, rare earth elements and refractory elements, whereas precious and base metals were digested in aqua regia. Prepared sample was mixed with $LiBO_2$/$Li_2B_4O_7$ flux. Crucibles are fused in a furnace. The cooled bead is dissolved in ACS grade nitric acid and analysed by ICP-OES and/or ICP-MS. Loss on ignition (LOI) is determined by igniting a sample split then measuring the weight loss. Total Carbon and Sulphur may be included and is determined by the Leco method (TC003). The LF202 package includes an additional 14 elements from an aqua regia digestion AQ200 to provide Au and volatile elements which do not report as part of the LF200 package. Representative data are shown in Table 1.

### 4.3. Electron Microprobe Analyses

The polished thin sections from four samples were prepared by the EAS Thin Section Laboratory at the Department of Earth and Atmospheric Sciences (EAS) at the University of Alberta. Major element compositions of minerals and phase relationships were studied by electron microprobe at the EAS at the University of Alberta (Canada). The operating conditions were; 40 degrees take off angle, accelerating voltage 20 kV, beam current 20 nA, and beam diameter < 1 micron (fully focused), except on the zeolite points that were run separately with a 10 micron diameter beam. The Kα X-ray lines of 13 elements were measured using the following diffraction crystals: PET (pentaerythritol) – P, K, Ca, Ti, V, Cr; TAP (thallium hydrogen phthalate) – Na, Mg, Al, Si; LIF (lithium fluoride) – Mn, Fe, Ni. Total count times of 30 seconds were used for both emission peaks and background positions for all elements except Na, for which 60 seconds was used. Interference corrections were applied to V for interference by Ti, and to Cr for interference by V, and to Mn for interference by Cr (Donovan et al., 1993). Intensity data were reduced according to Armstrong (1988) and the choice of mineral standards varied with the mineral analysed. Oxygen was calculated by stoichiometry and included in the data reduction. The investigated amphiboles structural formulae have been calculated through the ACES2013 Excel spreadsheet of Locock (2014). Representative mineral data are shown in Tables S2–S5 of the electronic supplementary material.

### 4.4. LA-ICP-MS Zircon U-Pb Analyses

Zircon for U-Pb dating was separated from jaw crushed and milled rock samples using a Wilfley shaker table, followed by magnetic and heavy liquid ($CHBr_3$ and CH2I2) separation. Then the zircon crystals were hand-picked under a binocular microscope and thermally annealed at 900 ℃ for 48 h in a muffle and afterwards fixed in epoxy resin and polished. Mineral separation and sample preparation were done at the Department

**Table 1.** Major, trace and rare earth element analyses of the felsic volcanic rocks of MAC

| Sample | AN-1 | AN-2 | AN-3 | AN-9 | AN-11 | AN-13 | AN-12 | AN-5 | AN-14 | AN-7 | AN-4 | AN-22 |
|---|---|---|---|---|---|---|---|---|---|---|---|---|
| $SiO_2$ | 68.55 | 67.93 | 69.17 | 69.57 | 69.06 | 68.28 | 69.11 | 68.42 | 69.19 | 69.28 | 68.32 | 68.7 |
| $Al_2O_3$ | 15.5 | 15.59 | 15.46 | 15.38 | 15.02 | 16.78 | 15.88 | 14.4 | 14.22 | 15 | 15.02 | 14.92 |
| $Fe_2O_3$ | 2.89 | 3.03 | 2.7 | 2.51 | 2.77 | 2.57 | 2.73 | 2.25 | 3.22 | 3.08 | 3.2 | 2.78 |
| MgO | 1.26 | 1.36 | 1.05 | 0.97 | 1.14 | 0.7 | 1.01 | 0.8 | 0.7 | 1.05 | 1.1 | 1.05 |
| CaO | 2.69 | 2.78 | 2.54 | 2.5 | 2.68 | 2.98 | 2.74 | 2.92 | 2.99 | 2.87 | 2.74 | 3.34 |
| $Na_2O$ | 4.23 | 4.22 | 4.28 | 4.42 | 4.19 | 4.09 | 3.98 | 4.98 | 3.33 | 3.31 | 4.38 | 4.27 |
| $K_2O$ | 3.19 | 3.18 | 3.3 | 3.3 | 2.82 | 2.99 | 2.66 | 3.78 | 3.73 | 3.03 | 3.26 | 3.29 |
| $TiO_2$ | 0.33 | 0.33 | 0.32 | 0.3 | 0.31 | 0.45 | 0.31 | 0.39 | 0.33 | 0.32 | 0.39 | 0.38 |
| Ti | 1978.35 | 1978.35 | 1918.4 | 1798.5 | 1858.45 | 2697.75 | 1858.45 | 2350.04 | 1978.35 | 1918.4 | 2338.05 | 2278.1 |
| $P_2O_5$ | 0.1 | 0.09 | 0.09 | 0.1 | 0.1 | 0.2 | 0.09 | 0.1 | 0.2 | 0.2 | 0.3 | 0.09 |
| MnO | 0.06 | 0.06 | 0.05 | 0.04 | 0.06 | 0.07 | 0.08 | 0.05 | 0.06 | 0.07 | 0.08 | 0.09 |
| Ba | 590 | 598 | 593 | 581 | 572 | n.a. | n.a. | n.a. | n.a. | n.a. | n.a. | n.a. |
| Ni | 28 | < | < | < | < | n.a. | n.a. | n.a. | n.a. | n.a. | n.a. | n.a. |
| Sc | 4 | 5 | 4 | 4 | 4 | n.a. | n.a. | n.a. | n.a. | n.a. | n.a. | n.a. |
| LOI | 1 | 1.3 | 0.9 | 0.8 | 1.7 | 0.8 | 1.1 | 1.6 | 1.8 | 1.5 | 1.2 | 1 |
| Total | 99.92 | 99.91 | 99.92 | 99.92 | 99.92 | 99.95 | 99.72 | 99.73 | 99.75 | 99.71 | 99.96 | 99.85 |
| Be | < | 3 | 3 | 2 | < | n.a. | n.a. | n.a. | n.a. | n.a. | n.a. | n.a. |
| Co | 5.7 | 6.4 | 5 | 4.3 | 5.3 | n.a. | n.a. | n.a. | n.a. | n.a. | n.a. | n.a. |
| Cs | 0.8 | 0.9 | 0.8 | 1 | 0.7 | n.a. | n.a. | n.a. | n.a. | n.a. | n.a. | n.a. |
| Ga | 13.4 | 15 | 14.3 | 14.3 | 14.3 | n.a. | n.a. | n.a. | n.a. | n.a. | n.a. | n.a. |
| Hf | 3.2 | 3.1 | 3.4 | 3 | 3.5 | n.a. | n.a. | n.a. | n.a. | n.a. | n.a. | n.a. |
| Nb | 12.8 | 12.2 | 12.1 | 12 | 12.7 | n.a. | n.a. | n.a. | n.a. | n.a. | n.a. | n.a. |
| Rb | 61.8 | 62.2 | 63.6 | 60.1 | 56.3 | n.a. | n.a. | n.a. | n.a. | n.a. | n.a. | n.a. |
| Sn | < 1 | < 1 | < 1 | < 1 | < 1 | n.a. | n.a. | n.a. | n.a. | n.a. | n.a. | n.a. |
| Sr | 235.2 | 245.8 | 230.5 | 230.2 | 207.3 | n.a. | n.a. | n.a. | n.a. | n.a. | n.a. | n.a. |
| Ta | 1.2 | 1 | 1.1 | 1.2 | 1.2 | n.a. | n.a. | n.a. | n.a. | n.a. | n.a. | n.a. |
| Th | 12.6 | 12.2 | 11.8 | 11.5 | 11.3 | n.a. | n.a. | n.a. | n.a. | n.a. | n.a. | n.a. |
| U | 2.1 | 2.1 | 2.1 | 2.3 | 2.3 | n.a. | n.a. | n.a. | n.a. | n.a. | n.a. | n.a. |
| V | 45 | 44 | 37 | 40 | 41 | n.a. | n.a. | n.a. | n.a. | n.a. | n.a. | n.a. |
| W | 1.3 | 0.9 | 0.6 | 0.6 | 0.5 | n.a. | n.a. | n.a. | n.a. | n.a. | n.a. | n.a. |
| Zr | 110.6 | 114.5 | 127.2 | 107.7 | 126.6 | n.a. | n.a. | n.a. | n.a. | n.a. | n.a. | n.a. |
| Y | 13.9 | 14.6 | 13.8 | 13.7 | 14.1 | n.a. | n.a. | n.a. | n.a. | n.a. | n.a. | n.a. |
| La | 27.2 | 27.1 | 27.6 | 28 | 24.5 | 23.5 | 25.3 | 26.6 | 27.7 | 27.4 | 26.9 | 27 |
| Ce | 46.9 | 46.2 | 47.4 | 45.5 | 42.4 | 44.1 | 47.3 | 43.3 | 49 | 46.3 | 44.5 | 48.4 |
| Pr | 4.51 | 4.57 | 4.46 | 4.55 | 4.31 | 4.22 | 4.12 | 4.51 | 5.04 | 4.42 | 5.27 | 5.2 |
| Nd | 14.7 | 15.1 | 15.2 | 14.7 | 14.5 | 15.7 | 16.1 | 12.4 | 16.1 | 16.9 | 17.2 | 14.2 |
| Sm | 2.61 | 2.69 | 2.39 | 2.36 | 2.44 | 2.77 | 2.38 | 2.39 | 1.81 | 3.31 | 2.25 | 3.01 |
| Eu | 0.62 | 0.61 | 0.6 | 0.59 | 0.6 | 0.61 | 0.83 | 0.62 | 0.62 | 0.8 | 0.39 | 0.55 |
| Gd | 2.35 | 2.51 | 2.25 | 2.24 | 2.37 | 1.92 | 2.79 | 2.35 | 3.12 | 3.05 | 2.01 | 3.4 |
| Tb | 0.37 | 0.36 | 0.35 | 0.33 | 0.37 | 0.32 | 0.31 | 0.31 | 0.33 | 0.4 | 0.32 | 0.55 |
| Dy | 2.18 | 2.36 | 2.23 | 2.16 | 2.35 | 2.53 | 2.01 | 2.48 | 2.25 | 2.87 | 2.53 | 1.99 |
| Ho | 0.46 | 0.44 | 0.41 | 0.45 | 0.46 | 0.44 | 0.41 | 0.56 | 0.41 | 0.43 | 0.42 | 0.42 |
| Er | 1.37 | 1.5 | 1.37 | 1.28 | 1.48 | 1.26 | 1.13 | 1.36 | 1.38 | 1.53 | 1.49 | 1.26 |
| Tm | 0.21 | 0.22 | 0.2 | 0.2 | 0.22 | 0.21 | 0.2 | 0.21 | 0.19 | 0.19 | 0.2 | 0.21 |
| Yb | 1.51 | 1.54 | 1.48 | 1.43 | 1.55 | 1.44 | 1.6 | 1.72 | 1.21 | 1.78 | 1.09 | 1.23 |
| Lu | 0.23 | 0.25 | 0.23 | 0.22 | 0.25 | 0.19 | 0.22 | 0.3 | 0.21 | 0.19 | 0.38 | 0.29 |
| Mo | 0.3 | 0.3 | 0.2 | 0.2 | 0.4 | n.a. | n.a. | n.a. | n.a. | n.a. | n.a. | n.a. |
| Cu | 2.3 | 2.8 | 2.1 | 1.9 | 6.7 | n.a. | n.a. | n.a. | n.a. | n.a. | n.a. | n.a. |
| Pb | 0.5 | 0.5 | 0.3 | 0.2 | 0.7 | n.a. | n.a. | n.a. | n.a. | n.a. | n.a. | n.a. |
| Zn | 22 | 22 | 19 | 14 | 38 | n.a. | n.a. | n.a. | n.a. | n.a. | n.a. | n.a. |
| Ni | 3.7 | 4.1 | 2.6 | 2.3 | 3.2 | n.a. | n.a. | n.a. | n.a. | n.a. | n.a. | n.a. |

<: Below detection limit; n.a: not analysed.


https://doi.org/10.1007/s12303-023-0027-4

of Geological Engineering, Çukurova University, Adana, Turkey. Cathodoluminescence (CL) and back-scattered (BSE) imaging was performed for identifying inherited cores, cracks and inclusions in the zircons using JEOL JSM-6610 LV SEM-EDS at the Geological Institute of the Bulgarian Academy of Sciences. The U-Pb zircon dating was performed at the LA-ICP-MS laboratory of the Geological Institute of the Bulgarian Academy of Sciences, using a New Wave UP193FX LA coupled to a Perkin Elmer ELAN DRC-e quadrupole ICP-MS. Laser parameters included ablation craters of 35 μm, an ablation frequency of 8 Hz and a detection time within 0.002–0.003 s. Analyses were calibrated with the GEMOC-GJ1 zircon (Jackson et al., 2004) as an external standard for fractionation correction. AusZ7 (Kennedy et al., 2014) and NIST610 (Jochum et al., 2007; Liu et al., 2010) zircons were used as unknowns or 'blind' sample, and used to correct systematic errors. Data reduction was processed using software Iolite v. 2.5 (Paton et al., 2011), applying down-hole fractionation correction to all the analyses. Diagram plots and concordia ages were obtained using Isoplot 4.15 (Ludwig, 2011).

## 5. RESULTS

### 5.1. Petrography and Mineralogy

The volcanic flows have been mainly dacite, rhyolite and relatively less extensively andesitic rocks. The following mineral assemblage consisting of plagioclase, quartz, biotite, amphibole, magnetite and ilmenite was studied in detail (Fig. 6a–e; Tables S3–S6 of the electronic supplementary material).

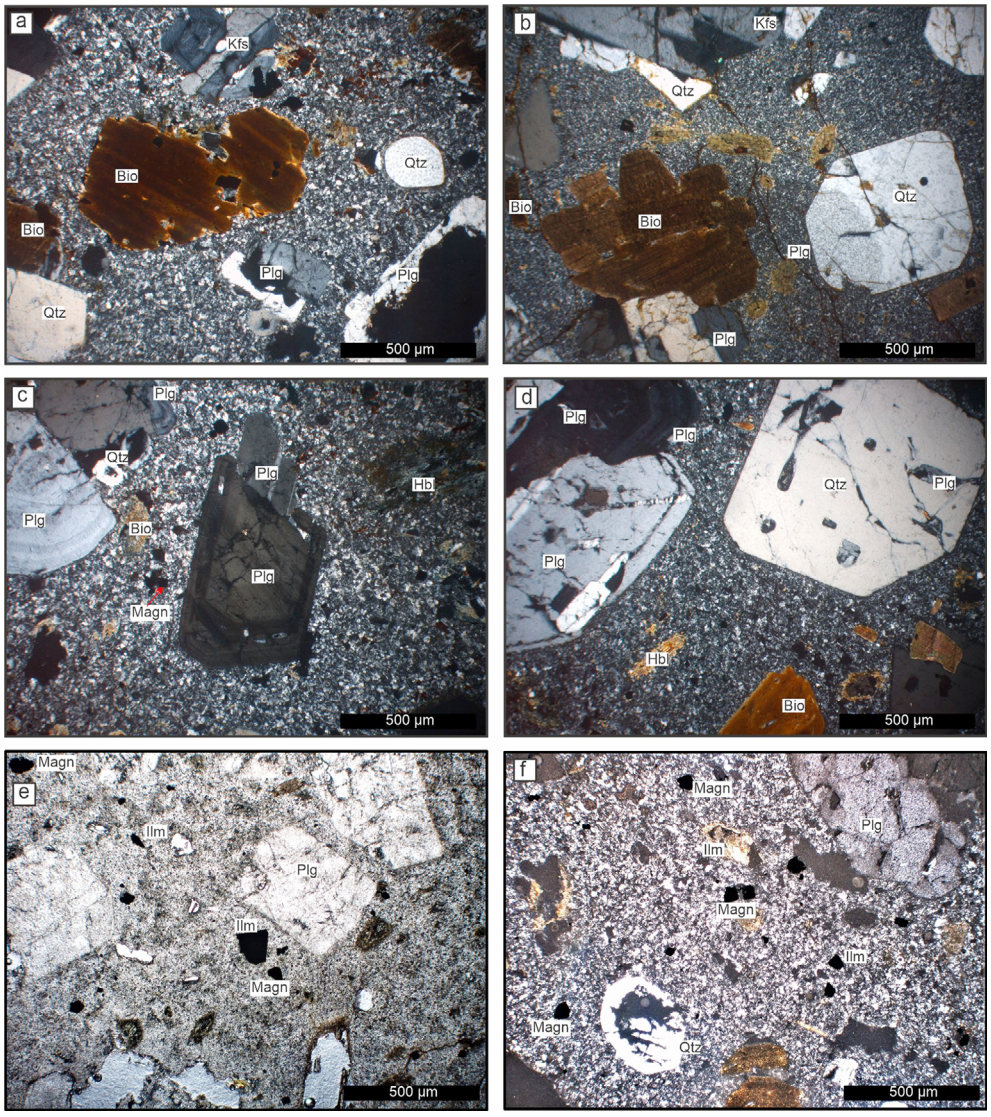



**Fig. 6.** Photomicrographs of volcanic rocks from the MAC in the Andirin region. (a) Microgranular porphyritic texture observed in rhyodacites. (b and d) Euhedral quartz crystals in rhyolite. (c) Appearance of hornblende and plagioclase crystals in dacite type volcanic rock. (e and f) The appearance of the primary magnetite and ilmenite minerals observed in the felsic volcanics of the Andirin region.

Among them, quartz and plagioclase phenocrysts are predominant, while ferromagnesian minerals such as biotite and amphibole are less commonly observed in the examined rocks. The rhyolitic and dacitic rocks present distinct characteristic petrographic properties.

The Andirin region volcanic rocks are dominantly dacite in association with rhyolite, and subordinate pyroclastic sequences (Fig. 6). The dacitic rocks present microlitic porphyritic, hyalo-microlitic, poikilitic and fluidal textures (Fig. 6a, b). Amphibole, plagioclase, biotite and titanite dominate these rocks, and dacitic lavas also have calcite, chlorite and sericite type secondary minerals. Plagioclases in the studied rocks form as microlites and euhedral and subhedral phenocrysts (Fig. 6). Poikilitic textures are also observed in some plagioclase ± quartz crystals. Irregular plagioclase edges have been developed because characteristically albite twinning and zoned plagioclases were crystallized together.

## 5.2. Mineral Chemistry Analyses

Two felsic volcanic samples have been selected to examine the mineral chemistry of investigated rocks. Calculated chemical

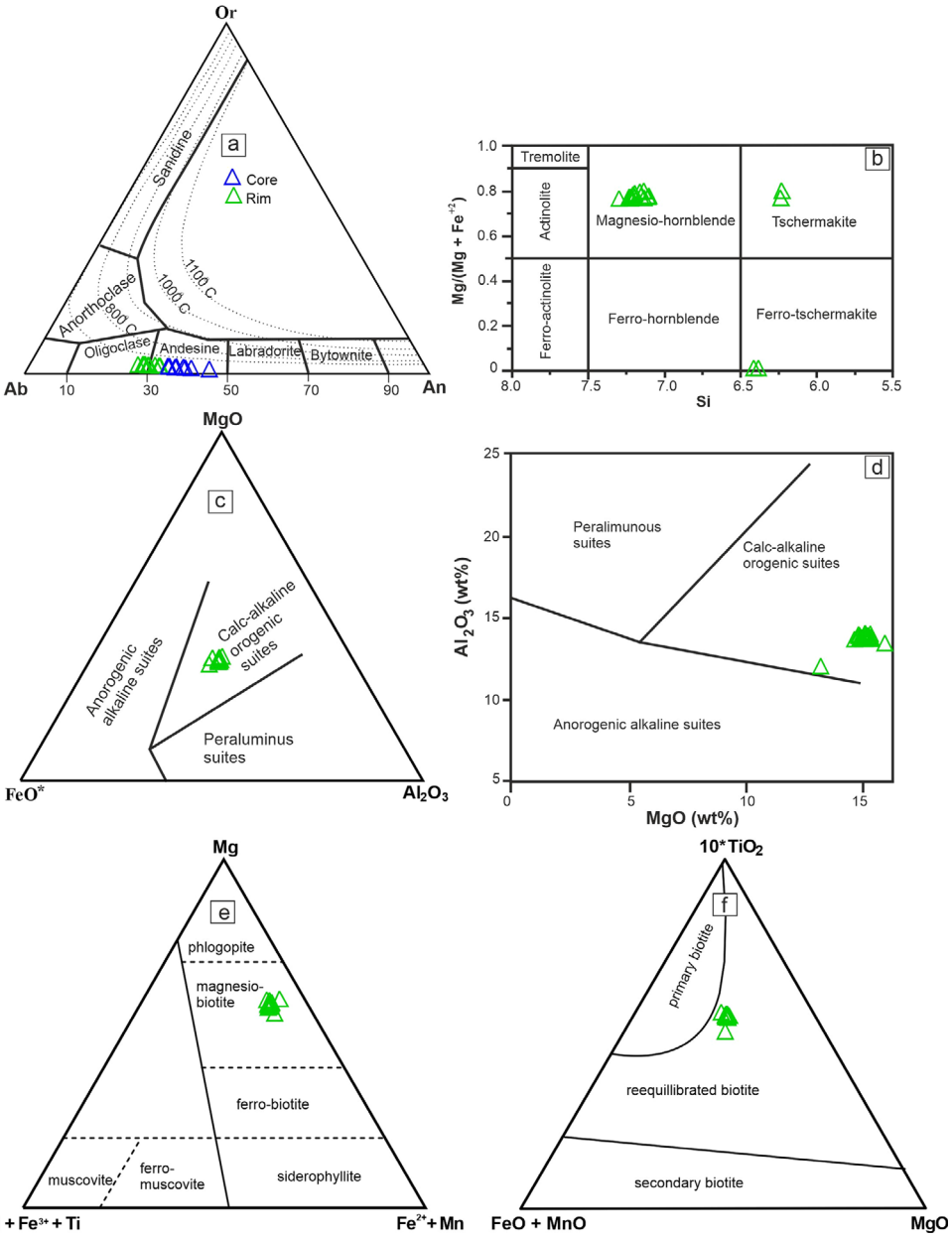



**Fig. 7.** (a) Classification of plagioclases (after Deer et al., 1992). (b) The mineral chemistry content of amphiboles in the felsic volcanic of the MAC (after Hawthorne at al., 2012). (c) MgO-$Al_2O_3$-FeO ternary classification diagram for biotite (after Abdel-Rahman, 1994). (d) $Al_2O_3$ versus MgO. (e) Ternary diagram of mica classification (after Nachit et al., 2005). (f) Chemical content of biotites using 10*$TiO_2$-(FeO + MnO)-MgO ternary diagram (after Foster, 1960).


https://doi.org/10.1007/s12303-023-0027-4

formulae of feldspar minerals and their representative contents are presented in Table S3 of the electronic supplementary material. In brief, the plagioclase compositions have been ranging from oligoclase to andesine together with $An_{(27–45)}$, $Ab_{(53–70)}$, and $Or_{(1–3)}$ in the classification diagram (Table S3; Fig. 7a). On the basis of the Hawthorne et al. (2012) diagram, the investigated amphibole crystals from felsic volcanic of the MAC are calcic characterise amphibole and are mainly defined as magnesio-hornblende and rare tschermakite/ferro-tschermakite (Fig. 7b). The analysed amphiboles were studied under mainly two groups. The magnesio-hornblende (first group) compositions from felsic volcanics of the MAC have been characterised by $SiO_2$ (49.21–50.76 wt%), $Al_2O_3$ (5.16–6.41 wt%), MnO (0.58–0.70 wt%), MgO (15.41–16.17 wt%), $Na_2O$ (1.02–1.21 wt%) and CaO (10.76–11.19 wt%) (Table S4 of the electronic supplementary material). Tschermakite/ferro-tschermakite (second group) contents from volcanics rocks are defined by $SiO_2$ (43.22–43.8 wt%), $TiO_2$ (2.06–20.56 wt%), $Al_2O_3$ (10.55–12.05 wt%), MnO (0.12–0.29 wt%), MgO (14.00–15.37 wt%), $Na_2O$ (2.10–2.27 wt%) and CaO (10.99–11.92 wt%) (Table S3). Structural formulae and chemical contents of analysed biotites are presented in Table S5 of the electronic supplementary material. The diagrams of Abdel-Rahman (1994) are able to discriminate the contents of mica especially biotite from the distinct geodynamic environments in terms of $Al_2O_3$, MgO, and FeO compositions. In the ternary and binary diagrams of Abdel-Rahman (1994), analysed biotite contents from felsic volcanics of the MAC are plotted in calc-alkaline orogenic suites (Fig. 7c, d). Analyzed biotite crystals give approximately equal FeO(t) (13.90–15.90 wt%) and MgO (13.32–15.88 wt%) compositions. The texture and content of investigated biotites present that these minerals are primary (re-equilibrated) igneous phases in whole sample data. This information is evidenced by plotting the compositions of analysed biotite crystals on the MgO-$TiO_2$-FeO(t) classification diagram (Nachit et al., 2005). In this classification diagram, the biotite contents indicate the mineral chemistry features associated with equilibrated primary igneous biotites (Fig. 7e). Mg number ratios (Mg/(Mg + Fe)) for biotite crystals present a narrow range and are from 0.62 to 0.66. When reflecting on the analysed data of biotite crystals in ($Fe^{2+}$ + Mn)-(Mg)-($Fe^{3+}$ + $Al^{VI}$ + Ti) classification (Fig. 7f), it has been presented that these crystals are magnesian biotite (Foster, 1960).

## 5.3. Oxygen Fugacities and Temperatures (Fe-Ti Oxides)

The oxides of ilmenite and magnetite can be used to estimate temperature and pressure status before eruption (Buddington and Lindsley, 1964; Frost et al., 1988; Frost, 1991). Typical contents of ilmenite and magnetite were obtained from analyses of 9 micro phenocrysts from two distinct region dacitic-rhyolitic rocks are presented in Table S6 of the electronic supplementary material. The oxides ilmenite and magnetite minerals have been analysed in examined volcanic samples AN9 and AN16 (rhyodacite), where those oxides can be found to be intergrown. After applying the Bacon and Hirschmann (1988) test for equilibrium, the data have been exported for use in Ghiorso and Evans (2008) geothermometer and oxygen barometer (Fig. 8). For sample AN9 (dacite), ilmenite-magnetite geothermobarometry indicates a median temperature of 732 ℃ at about 2.1 log units of oxygen fugacity above the fayalite-magnetite-quartz buffer (Table S6). For sample AN16 (based on fewer data), ilmenite-magnetite geothermobarometry indicates a median temperature of 698 ℃ at about 2.2 log units of oxygen fugacity above the fayalite-magnetite-quartz buffer (Table S6). According to Ghiorso and Evans (2008), the uncertainty due solely to analytical error is at least 50 ℃. The uncertainty has been expected in oxygen fugacity (delta FMQ) to be at least 0.1 log units. The ilmenite and magnetite analyses based on Fe-Ti oxide equilibria present that the Andirin region rhyodacitic and dacitic magmas were at 717 ℃ and at an $fO_2$ of approximately 2.16 log units (+1.51 NNO), which data show similar oxidized to Fish Canyon (Frost, 1991; Evans and Scaillet, 1997).

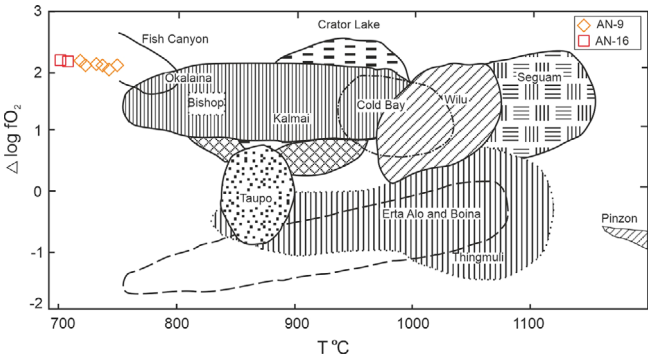



**Fig. 8.** Temperature versus oxygen fugacity diagram presenting the results from ilmenite and magnetite oxide geothermometry of Andirin region volcanic rocks. The diagram is adapted from Frost (1991).

## 5.4. U-Pb Zircon Dating

A striking aim of this paper is also to report crystallisation ages for felsic volcanic rocks of the Andirin region to set light on their temporal and spatial relationships. For this crucial purposes, LA-ICP-MS U/Pb zircon dating has been performed on felsic volcanic (dacite) samples (AN-2) and the geochronological data of the separated zircon crystals from the dacitic rocks were presented in supplementary material. The location of examined rocks has been given in Table S2 and Figure 9. The analytical procedures and sample preparation have been the same as

reported by Bonev et al. (2019a). Eighteen zircon crystals have been dated on nineteen credible U-Pb geochronological spots with 87–88% concordance were yielded. Examined zircon crystals present smooth and crack-free grain faces and have been 75–230 μm long with an average aspect ratio of 1.92. Anhedral zircon grains are rare on the contrary most crystals have been observed as euhedral to subhedral in shape (Fig. 9).

The examined zircon grains are pink, pale-brownish coloured, transparent and stubby in shape and these crystals present patchy growth oscillatory zoning and show isotropic, pyramidal shape. The Th/U ratios of the analysed crystals vary from 0.46 to 3.70, with the plurality of dated zircons having a moderate to high ratio of 0.46–0.87, which is typical for magmatic zircon crystals (Rubatto, 2002; Teipel et al., 2004). Nineteen spots out of eighteen zircons, fifteen spots of the core, and four spots from the rim, yielded Concordia age of 47.13 ± 0.50 Ma. (Fig. 9a; Table S1 of the electronic supplementary material).

## 5.5. Whole-rock Geochemistry

The whole-rock geochemistry data of the felsic volcanics from Andirin (Kahramanmaraş) are presented in Table 1. We chose samples that were minimally affected by hydrothermal alteration to obtain the primary compositions; whereas some

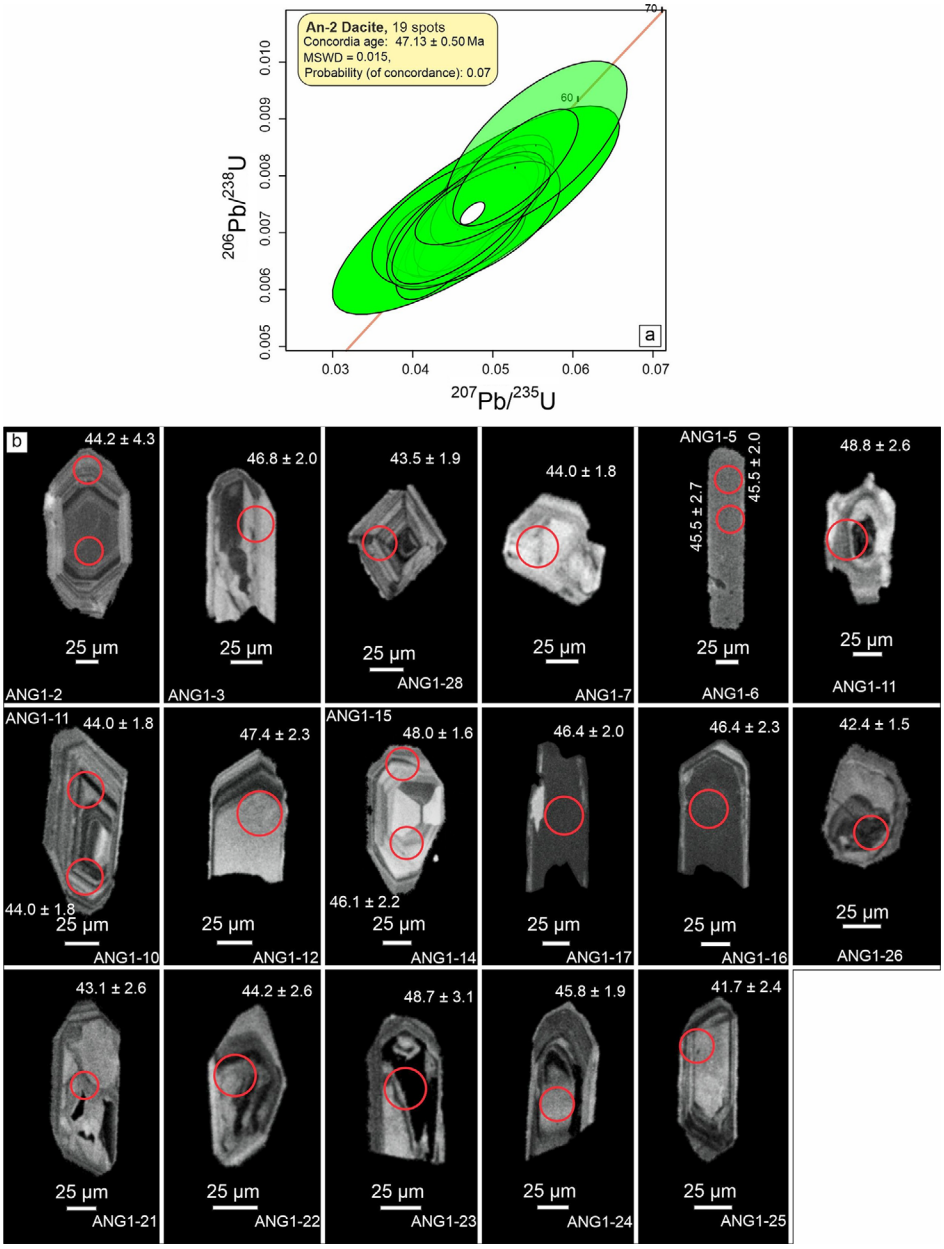



**Fig. 9.** (a) Plots of U-Pb zircon ages of the felsic volcanics of Andirin region (An-2). (b) Cathodoluminescence images (Cl) of analysed zircon crystals from dacites (An-2).


https://doi.org/10.1007/s12303-023-0027-4

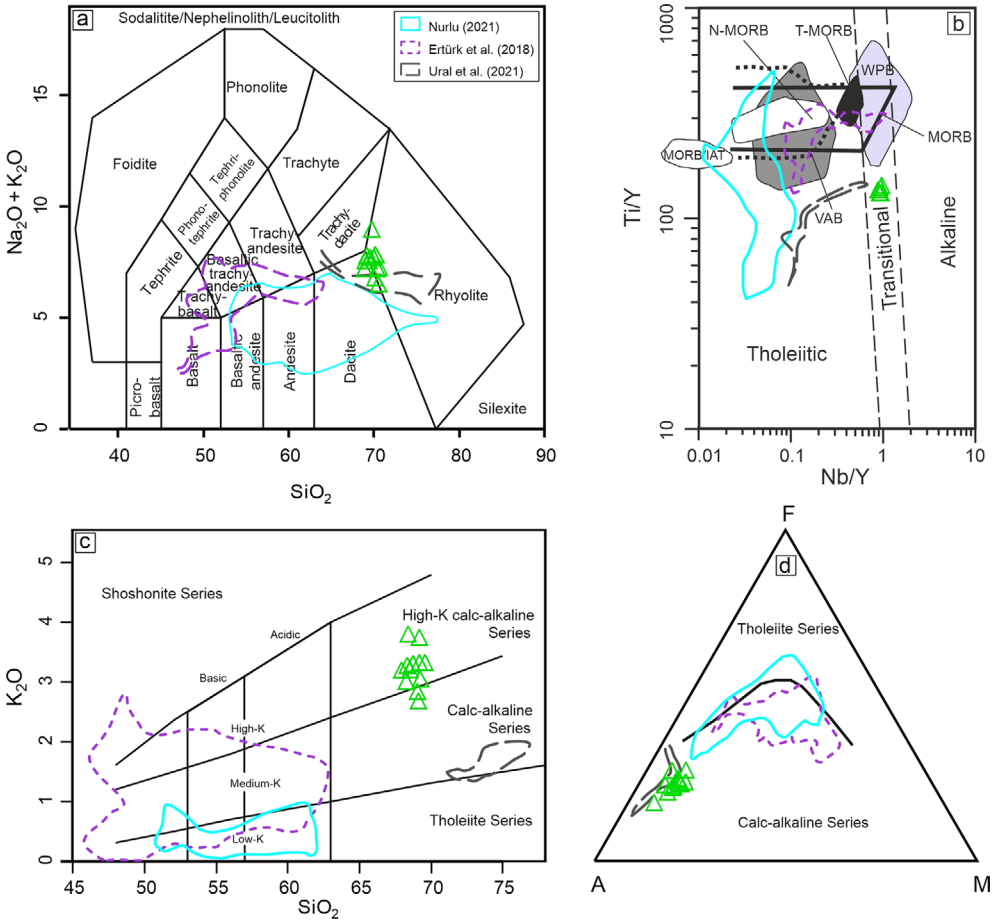



**Fig. 10.** (a) Plots of $SiO_2$ versus $Na_2O + K_2O$ (Total alkali versus Silica (TAS) diagram after Middlemost, 1994). (b) Nb/Y versus Ti/Y classification for felsic volcanic of the MAC. Modified from Pearce (1982). N-MORB, normal MORB; MORB/IAT, mid-oceanic ridge basalt/island arc tholeiite; WPB, within-plate basalts; VAB, volcanic arc basalt. (c) $SiO_2$ versus $K_2O$ diagram. The classification areas are taken from Peccerillo and Taylor (1976). (d) AFM classification of volcanic rocks from the MAC. The separation between calc-alkaline and tholeiitic subfields is taken from Irvine and Baragar (1971).

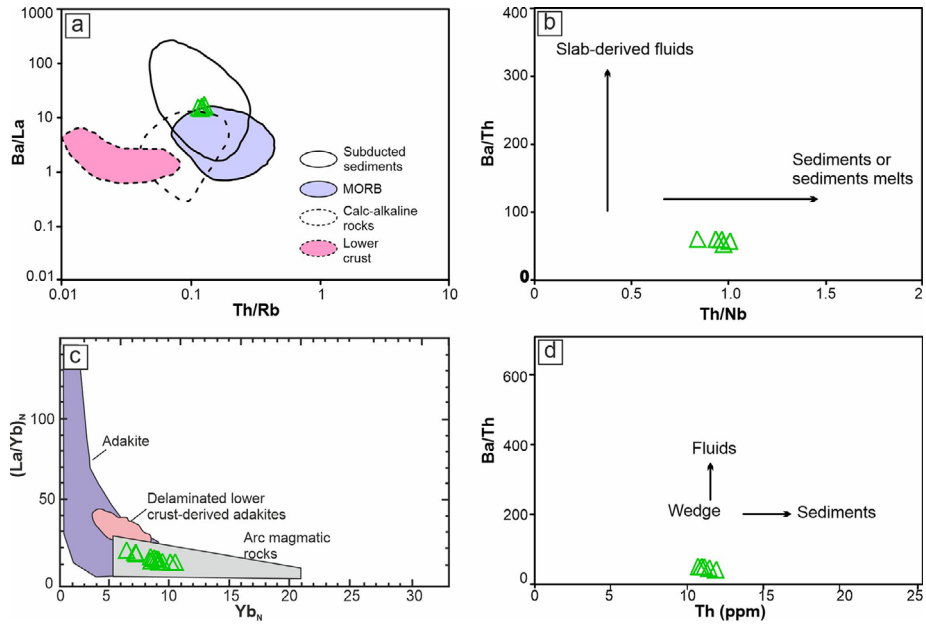



**Fig. 11.** Trace element data diagram. (a) Th/Rb versus Ba/La, (b) Th/Nb versus Ba/Th, (c) YbN versus La/YbN diagram (Defant and Drummond, 1990) for the examined rocks of MAC, (d) Th versus Ba/Th for felsic volcanics of Andirin region (subducted sediment contents are taken from Plank and Langmuir, 1998; Gill and Williams, 1990; McDermott and Hawkesworth, 1991).

secondary minerals (e.g., sericite, carbonate) form little contents of these rocks. The volcanic rocks of Andirin region are defined by high $SiO_2$ (67.93 to 69.57 wt%), $Na_2O$ (3.31 to 4.98 wt%), $K_2O$ (2.66 to 3.78 wt%) and $Al_2O_3$ (14.22 to 16.78 wt%) and low $Fe_2O_3$ (2.25 to 3.22 wt%) compositions. First, we plotted our felsic extrusive samples on the standard geochemical discrimination diagram of Middlemost (1994). The samples show variations in content rhyolite to dacite (Fig. 10a). The obvious transitional affinity of the felsic volcanic rocks of Andirin region is proven in the Nb/Y versus Ti/Y diagram of Figure 10b. Using the $SiO_2$ versus $K_2O$ diagram of Peccerillo and Taylor (1976) for the classification of the orogenic rock, the examined volcanic rocks present calc-alkaline and mainly high-K calc-alkaline series (Fig. 10c). In the AFM diagram of the major elements (Fig. 10d) there is a good correlation between examined rocks and these rocks fall calc-alkaline series subfield.

The Th/Rb versus Ba/La, Th/Nb versus Ba/Th and Th versus Ba/Th diagrams present that felsic volcanics of Andirin region plot toward subducted sediments and sediment melts which propose that the felsic volcanic of MAC had been primarily influenced by subducted sediment-derived magma and that slab-derived fluids had less effect on melts (Fig. 11a, b, d). The geochemistry of the felsic volcanics of MAC has been distinctive of arc magmatic (classical island arc) affinity. On $Yb_N$ versus $La_N/Yb_N$ diagram of Defant and Drummond (1990), compositions for the volcanic rocks plot in the arc magmatic subfield (Fig. 11c).

The felsic volcanic rocks of the MAC show marked light ion lithophile element (LILE) enrichment such as Cs, Ba, Rb, and K relative to high-field-strength elements (HFSE), in particular, Ti, Nb, and Sm, suggesting that these felsic rocks were formed in a subduction-related tectonic environment as island arc rocks (Fig. 12a). REE patterns of chondrite-normalized diagram of felsic volcanic rocks from the Andirin region are presented in Figure 12b. The examined dacitic-rhyolitic rocks are determinative of variable magmatic enrichment with spoon-like patterns [$(La/Yb)_N$ = 0.15–3.85], coupled with a prominent negative anomaly of Eu (Fig. 12b).

The significant negative anomaly of Eu in the dacitic-rhyolitic rocks of the MAC suggesting the removal of feldspars, in particular calcic-type, by fractional crystallisation and/or partial melting of rocks in that these plagioclases are held in the magma chamber (Rollison, 1993) (Fig. 12b). Alternatively, it may be related to variable degrees of oxygen fugacity in the mantle source (Burnham et al., 2015). The multi-element patterns (primitive mantle-normalized) of extrusive rocks from Andirin region are characterized by the enrichment of light rare earth elements (LILE) such as Th, La, Nd, Ce, and relative depletion of high field strength elements (HFSE) such as Ti, Nb and Ta, which attributes typical of the subduction zone environment (Wilson, 1989; Pearce, 2008) (Fig. 12c).

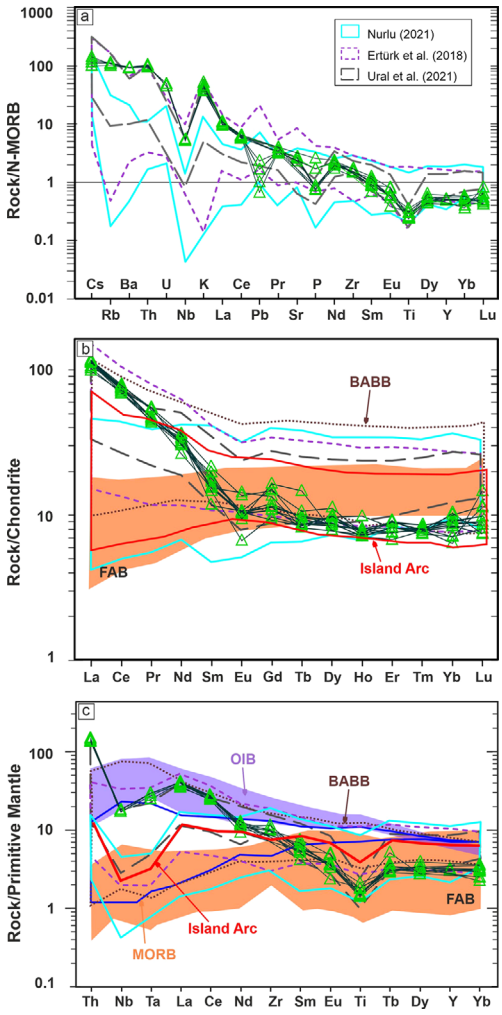



**Fig. 12.** (a) N-MORB-normalized multi-element trends of the felsic volcanic rocks from Andirin region. (b) Chondrite-normalized spider diagram of volcanics from the MAC. (c) Primitive mantle-normalized spider diagram. Petrological group and references: BABB, backarc basalts (Pearce et al., 2005; Buchs et al., 2013); FAB, forearc basalts (Reagan et al., 2010; Ishizuka et al., 2011); MORB, mid-ocean ridge basalts (Jenner and O'Neill, 2012); OIB, ocean island basalts (Willbold and Stracke, 2006; Buchs et al., 2013); Island arc basalts after Buchs et al. (2013). Comparison data for volcanic rocks observed in South-eastern Anatolia: Ertürk et al. (2018), Nurlu (2020), Ural et al. (2021).

The particular tectonic discrimination diagram was suggested by Shervais (1982) and this diagram depends on immobile elements such as $TiO_2$ versus V. Samples analysed from volcanic rocks show relatively low V and $TiO_2$ values and these extrusives are plotted into the arc field (Fig. 13a). In Ti versus Zr diagram of Pearce (1982), the felsic extrusives are plotted in evolved island arc (IA) subfield (Fig. 13b). In addition, in the geodynamic setting diagram reported by Pearce (2008), the extrusives are separated from the MORB-OIB array towards to the deep crustal recycling (Fig. 13c). In the Ta versus Nb variation diagram, the examined volcanics are defined by relatively low Ta/Nb compared


https://doi.org/10.1007/s12303-023-0027-4

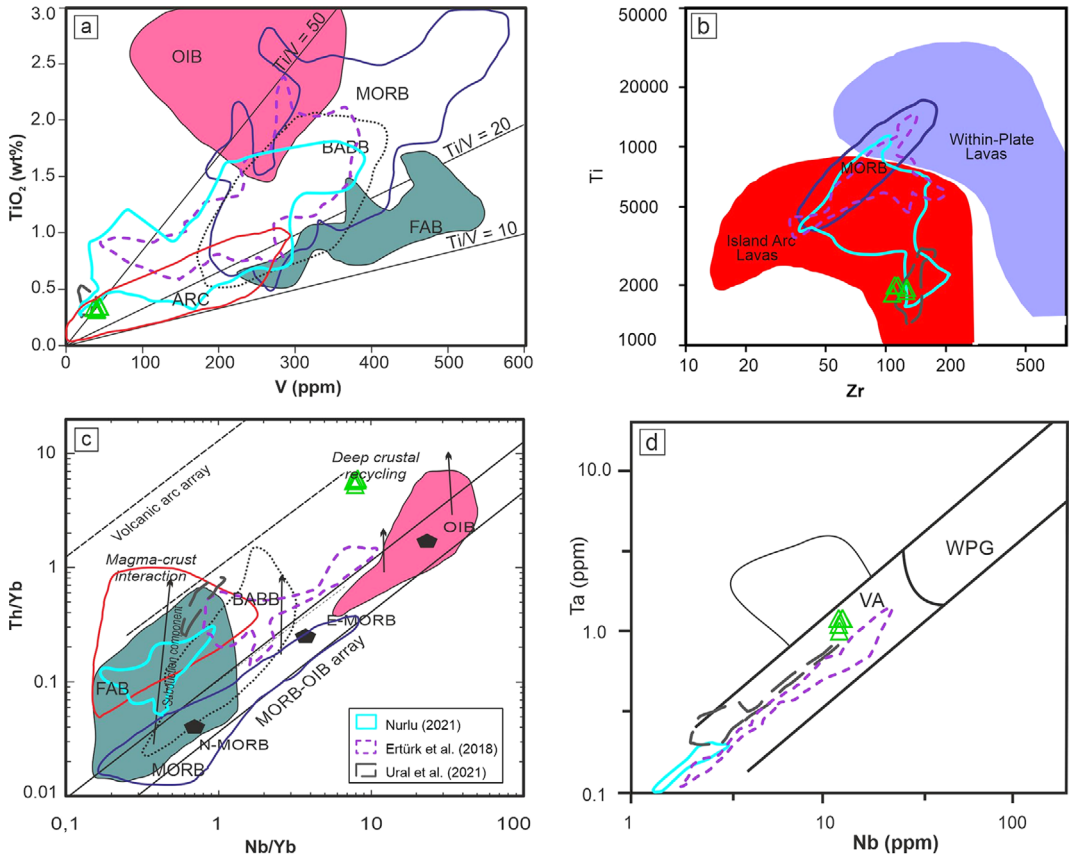



**Fig. 13.** (a) $TiO_2$ versus V (Shervais, 1982; Reagan et al., 2010). (b) Ti versus Zr diagram (Pearce, 1982) of felsic extrusives of Andirin region. (c) Th/Yb versus Nb/Yb (Pearce, 2008) discrimination diagram for the felsic extrusives of the MAC. (d) Ta versus Nb for felsic extrusives (after Harris et al., 1986).

to the WPG (within-plate granites) and these rocks are fallen primarily within VA (volcanic arc) subfield (Fig. 13d).

## 6. DISCUSSION

Generally, two fundamental petrological models were proposed for the genesis of volcanic rocks such as dacite and/or rhyolite (Allegre and Minster, 1978; Butler et al., 1997; Patiño Douce and McCarthy, 1998). The first one is partial melting of the lower continental crust and the second one is the fractional crystallization products of basaltic magma derived from the mantle. The geochemical data suggest that rhyolitic and dacitic rocks presumably were exposed to the same genetic treatments and have been more likely to be the effect of fractional crystallization from the same magmatic system.

### 6.1. Geodynamic Processes and Environment

The felsic, intermediate volcanics of the Andirin district include various extrusive rocks that range from andesite to rhyolite and are examined in this paper in detail for the first time in terms of geochemistry, geochronology and field relations. The existence of vesicles and fine-grained groundmass with prominent microgranular porphyritic and microlithic textures, propose shallow environment conditions for dacitic-rhyolitic rocks of the MAC.

While the felsic volcanics cropping out in the MAC are in an area with intense tectonics, the studied rocks have relatively low contents of water (LOI up to 1.8 wt%) therefore are rather fresh showing slight weathering. Pronounced correlations are observed between the immobile elements, such as REEs and HFSEs (e.g., Hf, Zr, Ta and Nb). The HFSEs and REEs are used to constrain the source characteristics and elucidate the petrogenetic processes of Andirin region felsic extrusives. Former studies have reported different formation processes for the occurrences of felsic rocks in a non-ridge environment, containing fractionation of mafic magmas (Yamamoto, 2007), assimilation of crustal materials into mantle-derived magmas (Crabtree and Lange, 2010; Frey and Lange, 2011) and crustal melting (Borg and Clynne, 1998). In volcanic rocks outcropping SE Anatolia, examined rocks and formerly reported extrusives (Nurlu et al., 2016; Ertürk et al., 2018) (Helete, Maden, etc.) present clear linear correlations on

Harker (1909) diagram which propose that relatively more felsic volcanics were derived from more basaltic parental magmas by fractional crystallization of magnetite, olivine, plagioclase and pyroxene (Fig. S1 of the electronic supplementary material). On the other hand, crustal mechanisms such as assimilation and crustal melting by original basaltic magmas could modify the geochemical content of the magma (Hildreth and Moorbath, 1988).

Mild negative Eu anomalies, whose patterns suggest plagioclase fractionation in the magma chamber, have been seen in all felsic volcanics. When evaluated in terms of M- to HREE tetrad effect observed in REE trends in Figure 12b; the obvious negative anomalies of Eu ratios in immensely evolved rocks such as examined felsic volcanic of the Andirin region propose that Eu fractionates among coexisting aqueous high-temperature fluid and/or the residual melt (Irber, 1999). Although the analysed volcanic rocks present very low LOI ratios (0.8–1.8 wt%), the obvious negative anomaly observed in the Eu element and the presence of tschermakite/ferro-tschermakite type secondary amphiboles suggest that the cause of the M- to HREE tetrad effect is hydrothermal alteration (Table 1; Fig. 12b). The felsic volcanics of MAC have been also defined by the diffuse existence of isotropic pseudomorphic development of secondary amphibole (tschermakite/ferro-tschermakite) over unaltered, not preserved Ca-inosilicate. Models of inverse geothermobarometry present tschermakite/ferro-tschermakite occurrences at 770 ℃ and 4.4–5.4 kbar, indicating limited high-temperature metasomatism disturbing the previously crystallized Ca-inosilicate. The La/Nb (1.92–2.33) and Nb/Th (1.0–1.12) ratios (Table 1) of all the samples from Andirin region present arc magmas or volcanic rocks affinity that could have been contributed by crustal source contents (Pearce, 1983; Wang et al., 2016). Furthermore, in the Th/Yb (7.29–8.34) and Ba/La (20.7–23.3) ratios, the analysed rocks yield nearly flat Ba/La ratios with relatively increasing Th/Yb, suggesting the contribution of sediments or crustal contamination (Pearce, 1983; Wang et al., 2016).

Micas especially biotite crystals are extensive hydrated ferromagnesian minerals in felsic, intermediate and mafic extrusive-intrusive rocks. These are delicate signs of compositional evolution in igneous rocks and physico-chemical conditions (Spear, 1984). The compositions of igneous biotites and their host magmas are related (Abdel-Rahman, 1994). The MgO, FeO and $Al_2O_3$ compositions of the biotite minerals could be to discriminate calc-alkaline, anorogenic alkaline from peraluminous (including S-type) (Abdel-Rahman, 1994). The MgO compositions of the biotite crystals in the felsic extrusive analysed range from 13.32 to 15.88 wt%, while the FeO compositions range from 13.90 to 15.90 wt% and the $Al_2O_3$ compositions from 12.05 to 14.16 wt% (Table S4). Evaluation of the triangular $Al_2O_3$-FeO-MgO diagram and binary MgO-$Al_2O_3$ diagram propose that the analysed biotite crystals from Andirin region plot in the subfield of calc-alkaline orogenic suites (Fig. 7). Abdel-Rahman (1994) reported that the average FeO*/MgO ratio of subduction-related calc-alkaline magma is 1.76 and accordingly the examined biotite crystals in this study yield similar ratios of FeO*/MgO (average = 0.98). Furthermore, the crystallization depth of the extrusive dacitic-rhyolitic rocks was defined from amphibole, magnetite and ilmenite chemistry content throughout this research. Typical igneous minerals found in hydrous calc-alkaline magmas that crystallize at deep are amphibole, magnetite and ilmenite. The mineral chemistry of magnetite, amphibole and ilmenite is sensitive to oxygen fugacity, pressure, water fugacity and temperature (Spear, 1981; Frost et al., 1988; Johnson and Rutherford, 1989; Frost, 1991). To tentatively evaluate the temperature and pressure setting of hornblende occurrences, we combine inverse geothermobarometry, as calculated from Pl-Hbl thermometry (Holland and Blundy, 1994; Anderson et al., 2008) and Al-in Hbl barometry (Schmidt, 1992; Anderson et al., 2008; Mutch et al., 2016). Data provided for inverse geothermobarometry models have been assessed via "weighted average" method in ISOPLOT 4.1 excel spreadsheet (Ludwig, 2003). Inverse geothermobarometry models given for examined amphiboles from extrusive rocks of the MAC a weighted average value of 1.79 ± 0.24 kb, ranging from 1.54 to 2.03 ± 0.50 kb for temperatures varying between 682 and 705 ± 40 ℃ (with a weighted mean value of 690 ± 20 ℃).

The MAC examined felsic extrusives are presented with relatively low MgO contents, and on the other hand have moderate silica values, which may have been sourced from mafic origins, either through fractional crystallisation or partial melting processes. All extrusive samples present relatively lower Zr/Nb ratios (ranging from 8.64 to 10.51) and these lower Zr/Nb ratios may be a result of partial melting and/or this may propose a derived from a more enriched source region (Sun and McDonough, 1989). The examined felsic rocks show relatively depleted Nb compositions over La and Th content and such features have been characteristics of magma occurrence in supra-subduction zone environment (e.g., Wilson, 1989; Pearce, 2008). Such as these geodynamic environments, then La and Th have been carried to the obducted mantle wedge through melts and hydrous fluids derived from the subducted plate (Elliott et al., 1997). The participation of subduction substances has been supported by the Th/Yb versus Nb/Yb diagram (Pearce, 2008), in which the examined rocks have been plotted deep crustal recycling (Fig. 13c). The primitive mantle-normalized (PM) multi-element diagram of studied rocks defines their marked certain enrichments, especially Th ($(Th)_{PM}$ = 132.9–148.2) and La ($(La)_{PM}$ = 35.6–40.7) where "P" indicates normalization to primitive mantle (PM-normalized values are taken from Sun


https://doi.org/10.1007/s12303-023-0027-4

and McDonough, 1989) see (Fig. 12c). Although the analysed felsic rocks appear to be generally compatible with the trace elements pattern of the island arc rocks, they show enrichment in Th, Nb, Ta, La and Ce. On the contrary, an obvious depletion is observed over island arc trends, especially in terms of Ti elements ($(Ti)_{PM}$ = 1.38–1.52). The analysed rocks presented clear negative anomalies that have been highlighted by their relatively high $(Th)_{PM}/(Nb)_{PM}$ (7.46–8.38) and $(La)_{PM}/(Nb)_{PM}$ (2.00–2.42). Accordingly, the analysed felsic extrusives exhibited clear enrichment in Light Rare Earth Elements (LREE) relative to heavy REE trends ($[La/Lu]_C$ = 7.24–14.46 in comparison to average chondrite according to Sun and McDonough, 1989). The prominent relatively high $(Th)_{PM}/(La)_{PM}$ (ranging from 3.32 to 3.74) ratios with regard to other HFSE and HREE, has been typically observed in the supra-subduction zone tectonic setting (arcs, back-arcs, etc.) (Pearce et al., 2005; Pearce and Stern, 2006). The Nb/Yb ratio of overall the felsic extrusives varies from 7.92 to 8.47 propose E-MORB source.

High calc-alkaline extrusives (rhyolites, andesites, dacites) have been characteristic magmas of convergent plate margin geodynamic environments. These rocks and studied rocks of MAC have been also defined by the enrichment of LILE (large ion lithophile elements), however present depletion in HFSE (high field strength elements) inducing a relatively negative anomaly in Ta-Nb in spider diagrams (Pearce, 1982). The chemical sign of these rocks has been mostly elucidated by the participation of flux of subducting sediment melts combined with fluids from the subducted oceanic lithosphere to the mantle wedge, causing magma occurrence and lowering the mantle solidus (Gill, 1981). Pitcher (1987) noted that high-K lavas erupted and emplaced in a continental arc environment analogue to the Andes. The isotopic features and chemistry of high-K, calc-alkaline magmatism in such a setting have been considered to mirror magma occurrence in mantle wedges that are enriched through interaction with sediments melts derived from subducted slabs similar to Andirin region volcanic rocks of MAC (Fig. 11). Characteristic trace elements and isotopic traces are created when crustally derived material is introduced to the parent, mantle-derived magma (Hildreth and Moorbath, 1988; Luhr, 1992).

The continental slab which is located southerly joined to the oceanic sliver underwent HP metamorphism and subducted together (Yılmaz, 2018). Partly simultaneously with this, the subducting oceanic slab got roll-back (retreated). As a result of this relatively hot asthenosphere wedged into the space constituted by the roll-back (Yılmaz, 2018) (Fig. 14). We inferred that the high-K volcanism of the Andirin region of MAC projects partial melting over the subducted slab and its southeastwardly oriented rollback that provoked migration of volcanic activity (Fig. 14). The asthenospheric input provided uncommonly high heat, which produced high temperature metasomatism, and the exhumation was also aided by the roll-back.

In the north-western part of the basin, coarse-blocked and chaotic olistostromal part of the Bulgurkaya formation were formed by gravity slips and ruptures, while the clastic dominated matrix material was deposited in slightly deeper sections. All the material was deformed by the effect of regional compression. Deformational and lithological characteristics of the Bulgurkaya Formation and the geological processes forming it, thought to have occurred during the transitional period from oceanic subduction to continental collision coinciding with the Eocene period in the region. Located on the Southeast Anatolian Orogenic Belt (SAOB), which can be considered the eastern extension of the Misis–Engizek Range, the Maden Basin, located about 200 km northeast of the studied area consisting of volcanic rocks represented mainly by basalt, andesite, and minor dacite that vary from low-K tholeiitic, calc-alkaline, high-K calc-alkaline in composition. They present enrichments in large ion lithophile and light rare earth elements and depletions in high field strength elements (Ertürk et al., 2018; Yılmaz et al., 2022). These geochemical characteristics are reported to indicate two end-members, a subduction-related mantle source and a continental crust, were involved in the magma genesis. The authors suggest that the Eocene Maden magmatism occurred as a post-collisional product by asthenospheric upwelling owing to convective removal of the lithosphere during an extensional collapse of the Southeast Anatolian ranges. Chen et al. (2022) reported that as is widely exposed in SE Turkey, Upper Cretaceous zircons were separated from granitoids associated with a coeval arc. Furthermore, the arc/back-arc magmatic rocks of the Maden Complex in SE Turkey are where Eocene zircons were derived (Chen et al., 2022). This study in the Andirin region reports that these volcanics with similar characteristics belong to the advanced stages of subduction. In addition, these units in Çağlayancerit and the Maden basin further north were highly tectonically amalgamated with other complex units in the following collisional periods, while they are relatively isolated and intact in the Andirin region. In the Çağlayancerit region (80 km east of Andirin), the volcanism of similar character must have probably occurred in the earlier period (Upper Cretaceous) (Akıncı et al., 2016), and these volcanic rocks in that region are seen as imbricated slices in the mélange units in front of the Bulgurkaya Formation in the thrust front. Ural et al. (2021) examined intermediate-felsic volcanic rocks of Elazığ region (SAOB) and they reported that Cretaceous-aged volcanic rocks gathered from five distinct places in the Elazığ city are low Nb/Y with subalkaline in character. Furthermore, they also noted that most of the analysed samples are chemically grouped as dacites/ryhodacites, while a rare percentage is seen to be andesitic rocks. Ural et al. (2021) also

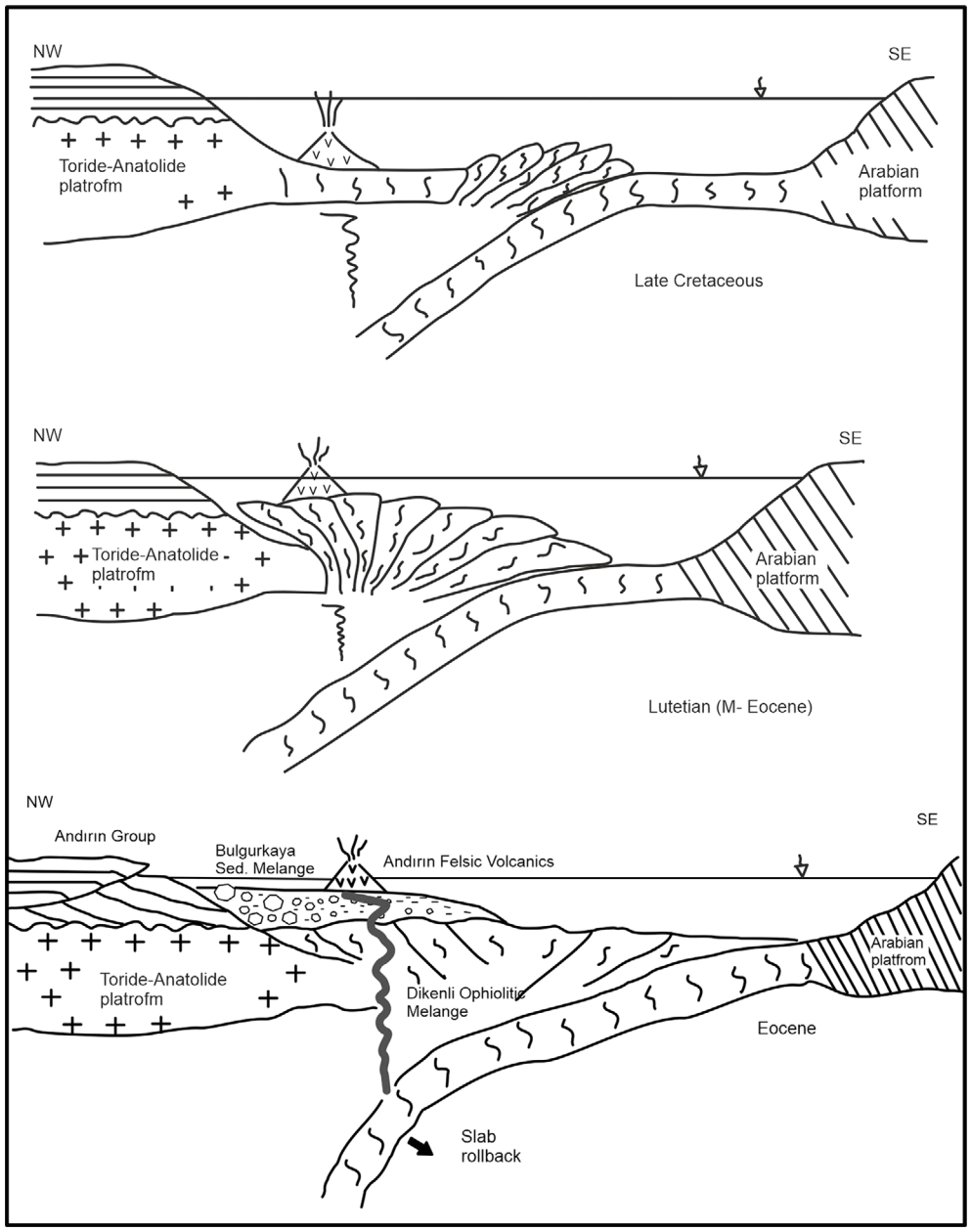



**Fig. 14.** Cartoons presenting the inferred Late Cretaceous–Middle Eocene geodynamic environment of the units in the area examined (modified from Yılmaz and Gürer, 1996; Yılmaz, 2018).

presented N-MORB-normalized spider diagram and they emphasized that these volcanic rocks have been defined by relative enrichments in La and Th over Zr, Ti, Nb and Hf, presenting their derivation from a subduction zone environment. Although the felsic volcanic rocks that are the subject of this paper are different from these extrusives in age, they show similarity in geochemical character. Sr-Nd isotope and whole rock major-trace-rare earth element data from Middle Eocene extrusives outcropped in Maden Complex (SAOB) were presented by Ertürk et al. (2018). They noted that these volcanics had been characterised by andesite, basalt and rare dacitic rocks that vary from calc-alkaline, low-K tholeiitic, shoshonitic and high-K calc-alkaline in content. The orogenic signs of the volcanic rocks of Maden Complex are featured to the mantle origin that probably has been metasomatized due to intraoceanic subduction of the southern branch of the Neo-Tethys in the Late Cretaceous (Ertürk et al., 2018). While the volcanic rocks of the Maden Complex and the felsic extrusive rocks of the Andirin region are of Eocene age, they differ in terms of geochemical characteristics. The Volcanic rocks, sheeted dikes and gabbros of Meydan ophiolite (east of study area) in SAOB had been studied to define their Nd-Sr-Pb isotope compositions, whole-rock, mineral


https://doi.org/10.1007/s12303-023-0027-4

chemistry and U-Pb zircon ages (Nurlu, 2020). The mineral chemistry and whole rocks geochemical data of the volcanic rocks of the Meydan–Helete region propose that these rocks were formed in a supra-subduction zone (Nurlu, 2020).

The dacitic-rhyolitic rocks, studied in the Andirin region are not very common along the Misis–Engizek extension and seem unique for the Andirin region of the MAC. These felsic volcanic rocks, which are observed intricately with the rich clastic matrix part of the Bulgurkaya Formation in the studied region, were probably emplaced in the foreland of the nappe zone in the north, in relation to the later stages of the subduction event in the southeast (Fig. 14).

There are no isotopic or radiometric age reports existing from the Andirin region, containing the felsic volcanics of MAC. The U-Pb zircon geochronology results presented in this research indicate the first comprehensive geochronology data from the volcanic of the Andirin region (MAC).

## 7. CONCLUSIONS

Field mapping, geochemical (whole-rock, mineral chemistry), and geochronological study of the felsic volcanics in relation to other units of the Andirin region (MAC) yielded the following conclusions:

- Besides the dominated felsic rhyolite-dacite rock types there were limited observed intermediate andesite rock types within the volcanic rocks of the Andirin region (SE Anatolia).
- Felsic volcanic rocks are intercalated with the olistostromal Bulgurkaya Fm. in the studied area.
- Whole-rock composition shows their medium- to high-K calc-alkaline character with enriched the LREE and depleted the HFSE relative to the primitive mantle, and together with their mineral chemistry indicate that felsic volcanics of the MAC were formed in a volcanic arc geodynamic environment, derived from the supra-subduction zone within the Misis-Andirin Complex.
- Laser ablation U-Pb zircon geochronology of the Andirin region volcanics (dacite) yielded a concordia $^{206}Pb/^{238}U$ age of 47.13 ± 0.5 Ma. The U-Pb analyses evaluated crystallization age and suggest that significant volcanism formed in the Middle Eocene (Lutetian), at roughly 47 Ma in the studied region.
- The magnetite and ilmenite mineral chemistry analyses based on Fe-Ti oxide equilibria present that the Andirin region volcanics were at 717 ℃ and at an $fO_2$ of approximately 2.16 log units (+1.51 NNO). The Al-in hornblende thermobarometry (2.04 to 1.55 kbar) of Mg-Fe hornblende in the felsic extrusive rocks of Andirin region represents their crystallization in the moderate to shallow crustal level at a maximum 6.7 km to a minimum 5.1 km depth.
- The U-Pb zircon dating yield crystallization ages of ca. 47.13 ± 0.5 Ma for felsic extrusives from the Andirin district of the MAC and this age data obtained reveal the Eocene-aged volcanic unit for the first time in the Misis-Andirin Complex and the Southeast Anatolian Orogenic Belt.
- The geochemical features of high-K, calc-alkaline magmatism in a continental arc setting have been considered to mirror magma occurrence in mantle wedges that are enriched through interaction with sediments melts derived from subducted slabs similar to Andirin region volcanic rocks of MAC.

## ACKNOWLEDGMENTS

We would like to thank Dr. Andrew Locock (Alberta University, Canada) for performing mineral chemistry analyses and Dr. Petyo Filipov (Bulgarian Academy of Sciences, Bulgaria) for LA-ICP-MS Zircon Analyses. We are highly grateful to Professor Serhat Köksal and an anonymous reviewer for their constructive comments, which helped us to improve our presentation. We also thank to Editor Professor Sung Hi Choi for careful editorial handling. English was checked by professionals from the Proof-reading Service company (www.proof-reading-service.com). The research was financially supported by the Cukurova University (Turkey) Research Foundation (Project No: FBA-2023-15770).

## REFERENCES

Abdel-Rahman, A.M., 1994, Nature of biotites from alkaline, calc-alkaline and peraluminous magmas. Journal of Petrology, 35, 525–541. https://doi.org/10.1093/petrology/35.2.525

Akıncı, A.C, Robertson, A.H.F., and Ünlügenç, U.V., 2016, Late Cretaceous–Cenozoic subduction-collision history of the Southern Neotethys: new evidence from the Çağlayancerit area, SE Turkey. International Journal of Earth Sciences, 105, 315–337. https://doi.org/10.1007/s00531-015-1199-6

Akıncı, A.C. and Ünlügenç, U.C., 2021, Neogene tectonic evolution of the Misis-Andirin-Engizek range: structural and sedimentary evidences from Bulgurkaya Sedimentary Mélange. Arabian Journal of Geosciences, 14, 1–23. https://doi.org/10.1007/s12517-021-06991-x

Aktaş, G. and Robertson, A.H.F., 1984, The Maden Complex, SE Turkey: evolution of a Neotethyan continental margin. In: Dixon, J.E. and Robertson, A.H.F. (eds.), The Geological Evolution of the Eastern Mediterranean. Geological Society, London, Special Publications, 17, p. 375–402. https://doi.org/10.1144/GSL.SP.1984.017.01.2

Allegre, C.J. and Minster, J.F., 1978, Quantitative method of trace element behavior in magmatic processes. Earth and Planetary Science Letters, 38, 1–25.

Anderson, J.L., Barth, A.P., Wooden, J.L., and Mazdab, F., 2008, Thermometers and thermobarometers in granitic systems. Reviews in Mineralogy and Geochemistry, 69, 121–142. https://doi.org/10.2138/rmg.2008.69.4

Armstrong, J.T., 1988, Quantitative analysis of silicates and oxide minerals: comparison of Monte Carlo, ZAF and φ (ρz) procedures. In: Newbury, D.E. (ed.), Microbeam Analysis. Quantitative Electron Probe Analysis, San Francisco Press, San Francisco, USA, p. 239–246.

Ayaslıoğlu, Y., 1970, Berke Project – Berke Dam Engineering Geology Planning Report. Directorate General for State Hydraulic Works (DSI). (Unpublished-in Turkish with English abstract)

Bacon, C.R. and Hirschmann, M.M., 1988, Mg/Mn partitioning as a test for equilibrium between coexisting Fe-Ti oxides. American Mineralogist, 73, 57–61.

Barrier, E. and Vrielynck, B., 2008, Palaeotectonic maps of the Middle East: tectono-sedimentary-palinspastic maps from Late Norian to Pliocene. Scale 1:18,500,000, Commission for the Geological Map of the World (CGMW), Paris, France, 14 p.

Beyarslan, M. and Bingöl, A.F., 2000, Petrology of a supra-subduction zone ophiolite (Kömürhan-Elazığ-Turkey). Canadian Journal of Earth Sciences, 37, 1411–1424. https://doi.org/10.1139/e00-041

Bonev, N., Filipov, P., Raicheva, R., Chiaradia, M., and Moritz, R., 2019, Detrital zircon age and Sr isotopic constraints for a Late Palaeozoic carbonate platform in the lower Rhodope thrust system, Pirin, SW Bulgaria. Geological Magazine, 156, 12. https://doi.org/10.1017/S0016756819001183

Borg, L.E. and Clynne, M.A., 1998, The petrogenesis of felsic calc-alkaline magmas from the southernmost Cascades, California: origin by partial melting of basaltic lower crust. Journal of Petrology, 39, 1197–1222. https://doi.org/10.1093/petroj/39.6.1197

Buchs, D.M., Bagheri, S., Martin, L., Hermann, J., and Arculus, R., 2013, Palaeozoic to Triassic ocean opening and closure preserved in central Iran: constraints from the geochemistry of meta-igneous rocks of the Anarak area. Lithos, 172–173, 267–287. https://doi.org/10.1016/j.lithos.2013.02.009

Buddington, A.F. and Lindsley, D.H., 1964, Iron-titanium oxide minerals and synthetic equivalents. Journal of Petrology, 5, 310–357.

Burnham, A.D., Berry, A.J., Halse, H.R., Schofield, P.F., Cibin, G., and Mosselmans, J.F.W., 2015, The oxidation state of europium in silicate melts as a function of oxygen fugacity, composition and temperature, Chemical Geology, 411, 248–259.

Butler, R.W.H., Harris, N.B.W., and Whittington, A.G., 1997, Interactions between deformation, magmatism, and hydrothermal activity during active crustal thickening: a field example from Nanga Parbat, Pakistan Himalayas. Mineralogical Magazine, 61, 37–68.

Chen, G., Robertson, A.H.F., and Wu, F.Y., 2022, Detrital zircon geochronology and related evidence from clastic sediments in the Kyrenia Range, N Cyprus: implications for the Mesozoic–Cenozoic erosional history and tectonics of southern Anatolia. Earth-Science Reviews, 233, 1–34. https://doi.org/10.1016/j.earscirev.2022.104167

Crabtree, S.M. and Lange, R.A., 2010, Complex phenocryst textures and zoning patterns in andesites and dacites: evidence of degassing-induced rapid crystallization. Journal of Petrology, 52, 3–38. https://doi.org/10.1093/petrology/egq067

Deer, W.A., Howie, R.A., and Zussman, J., 1992, An Introduction to the Rock Forming Minerals (2nd edition). Prentice Hall, Harlow, UK, 696 p.

de Hoog, J.C.M., Mason, P.R.D., and van Bergen, M.J., 2001, Sulfur and chalcophile elements in subduction zones: constrains from a laser ablation ICP-MS study of melt inclusions from Galunggung Volcano, Indonesia. Geochimica et Cosmochimica Acta, 65, 3147–3164. https://doi.org/10.1016/S0016-7037(01)00634-2

Defant, M. and Drummond, M.S., 1990, Derivation of some modern arc magmas by melting of young subducted lithosphere. Nature, 347, 662–665. https://doi.org/10.1038/347662a0

Dewey, J.F., Hempton, M.R., Kidd, W.S.F., Şaroğlu, F., and Şengör, A.M.C., 1986, Shortening of continental lithosphere: the neotectonics of Eastern Anatolia – a young collision zone. In: Coward, M.P. and Ries, A.C. (eds.), Collision Tectonics. Geological Society, London, Special Publications, 19, p. 3–36. https://doi.org/10.1144/GSL.SP.1986.019.01.01

Dilek, Y. and Furnes, H., 2019, Tethyan ophiolites and Tethyan seaways. Journal of the Geological Society, 176, 899–912. https://doi.org/10.1144/jgs2019-129

Dilek, Y. and Sandvol, E., 2009, Seismic structure, crustal architecture and tectonic evolution of the Anatolian-African plate boundary and Cenozoic orogenic belts in the eastern Mediterranean region. In: Murphy, J.R., Keppie, J.D., and Hynes, A.J. (eds.), Ancient Orogens and Modern Analogues. Geological Society, London, Special Publications, 327, p. 127–160. https://doi.org/10.1144/SP327.8

Donovan, J.J., Snyder, D.A., and Rivers, M.L., 1993, An improved interference correction for trace element analysis. Microbeam Analysis, 2, 23–28.

Duman, T.Y., Robertson, A.H.F., Elmacı, H., and Kara, M., 2017, Palaeozoic–Recent geological development and uplift of the Amanos Mountains (S Turkey) in the critically located northwesternmost corner of the Arabian continent. Geodinamica Acta, 29, 103–138. https://doi.org/10.1080/09853111.2017.1323428

Elliott, T., Plank, T., Zindler, A., White, W., and Bourdon, B., 1997, Element transport from slab to volcanic front in the Mariana arc. Journal of Geophysical Research, 780, 14991–15019. https://doi.org/10.1029/97JB00788

Ertürk, M.A., Beyarslan, M., Chung, S.L., and Lin, T.H., 2018, Eocene magmatism (Maden complex) in the Southeast Anatolian Orogenic Belt: magma genesis and tectonic implications. Geoscience Frontiers, 9, 1829–1847. https://doi.org/10.1016/j.gsf.2017.09.008

Evans, B.W. and Scaillet, B., 1997, The redox state of Pinatubo dacite and the ilmenite-hematite solvus. American Mineralogist, 82, 625–629. https://doi.org/10.2138/am-1997-5-621

Floyd, P.A., Kelling, G., Gökçen, S.L., and Gökçen, N., 199l, Geochemistry and tectonic environment of basaltic rocks from the Misis ophiolitic melange, south Turkey. Chemical Geology, 89, 263–280. https://doi.org/10.1016/0009-2541(91)90020-R

Foster, M.D., 1960, Interpretation of composition of trioctaheral micas. USGS Professional Paper, 354-B, U.S. Geological Survey, 49 p. https://doi.org/10.3133/pp354B

Frey, H.M. and Lange, R.A., 2011, Phenocryst complexity in andesites and dacites from the Tequila Volcanic Field, Mexico: resolving the effects of degassing vs. magma mixing. Contributions to Mineralogy and Petrology, 162, 415–445. https://doi.org/10.1007/s00410-010-0604-1

Frost, B.R., 1991, Introduction to oxygen fugacity and its petrologic importance. In: Lindsley, D.H. (ed.), Oxide Minerals: Petrologic and

Magnetic Significance. Reviews in Mineralogy, 25, p. 1–9. https://doi.org/10.1515/9781501508684-004

Frost, B.R., Lindsley, D.H., and Andersen, D.J., 1988, Fe-Ti oxide-silicate equilibria: assemblages with fayalitic olivine. American Mineralogist, 73, 727–740

Furman, T., Hanan, B.B., Sjoblom, M.P., Kürkcüoğlu, B., Sayit, K., Şen, E., Alıcı Şen, P., and Yürür, T., 2021, Evolution of mafic lavas in central Anatolia: mantle source domains. Geosphere, 17, 1631–1646. https://doi.org/10.1130/GES02329.1

Gall, H., Furman, T., Hanan, B., Kürkcüoğlu, B., Sayıt, K., Yürür, T., Sjoblom, M.P., Şen, E., and Alıcı Şen, P., 2021, Post-delamination magmatism in south-central Anatolia. Lithos, 398–399, 106299. https://doi.org/10.1016/j.lithos.2021.106299

Ghiorso, M.S. and Evans, B.W., 2008, Thermodynamics of rhombohedral oxide solid solutions and a revision of the FE-TI two-oxide geothermometer and oxygenbarometer. American Journal of Science, 308, 957–1039.

Gill, J.B., 1981, Orogenic Andesites and Plate Tectonics. Springer, Berlin, 390 p. https://doi.org/10.1007/978-3-642-68012-0

Gill, J.B. and Williams, R.W., 1990, Th isotope and U-series studies of subduction-related volcanic rocks. Geochimica et Cosmochimica Acta, 54, 1427–1442.

Gökçen, S.L., Kelling, G., Gökçen, N., and Floyd, P.A., 1988, Sedimentology of a late Cenozoic collisional sequence: the Misis Complex, Adana, southern Turkey. Sedimentary Geology, 59, 205–235.

Hall, R., 1976, Ophiolite emplacement and the evolution of the Taurus suture zone, South-east Turkey. Geological Society of America Bulletin, 87, 1078–1088.

Harker, A., 1909, The Natural History of Igneous Rocks. Methuen & Co., London, UK, 384 p.

Harris, N.B.W., Pearce, J.A., and Tindle, A.G., 1986, Geochemical characteristics of collision zone magmatism. In: Coward, M.P. and Ries, A.C. (eds.), Collision Tectonics. Geological Society, London, Special Publications, 19, p. 67–81. https://doi.org/10.1144/GSL.SP.1986.019.01.04

Hawthorne, F.C., Obertii, R., Harlow, G.E., Maresch, W.V., Martin, R.F., Schumacher, J.C., and Welch, M.D., 2012, Nomenclature of the amphibole supergroup. American Mineralogist, 97, 2031–2048. https://doi.org/10.2138/am.2012.4276

Hildreth, W. and Moorbath, S., 1988, Crustal contributions to arc magmatism in the Andes of central Chile. Contributions to Mineralogy and Petrology, 98, 455–489. https://doi.org/10.1007/BF00372365

Holland, T. and Blundy, J., 1994, Non-ideal interactions in calcic amphiboles and their bearing on amphibole-plagioclase thermometry. Contributions to Mineralogy and Petrology, 116, 433–447. https://doi.org/10.1007/BF00310910

Irber, W., 1999, The lanthanide tetrad effect and its correlation with K/Rb, Eu/Eu?, Sr/Eu, Y/Ho, and Zr/Hf of evolving peraluminous granite suites. Geochimica et Cosmochimica Acta, 63, 489–508. https://doi.org/10.1016/S0016-7037(99)00027-7

Irvine, T.N. and Baragar, W.R.A., 1971, A guide to the chemical classification of the common volcanic rocks. Canadian Journal of Earth Sciences, 8, 523–548.

Ishizuka, O., Tani, K., Reagan, M.K., Kanayama, K., Umino, S., Harigane, Y., Sakamoto, I., Miyajima, Y., Yuasa, M., and Dunkley, D.J., 2011, The timescales of subduction initiation and subsequent evolution of an oceanic island arc. Earth and Planetary Science Letters, 306, 229–240. https://doi.org/10.1016/j.epsl.2011.04.006

Jackson, S.E., Pearson, N.J., Griffin, W.L., and Belousova, E.A., 2004, The application of laser ablation-inductively coupled plasma-mass spectrometry to in situ U-Pb zircon geochronology. Chemical Geology, 211, 47–69. https://doi.org/10.1016/j.chemgeo.2004.06.017

Jenner, F.E. and O'Neill, H.S.C., 2012, Analysis of 60 elements in 616 ocean floor basaltic glasses. Geochemistry, Geophysics, Geosystems, 13, 1–11. https://doi.org/10.1029/2011GC004009

Jochum, K., Stoll, B., Herwig, K., and Willbold, M., 2007, Validation of LA-ICP-MS trace element analysis of geological glasses using a new solid-state 193 nm Nd: YAG laser and matrix-matched calibration. Journal of Analytical Atomic Spectrometry, 22, 112–121.

Johnson, M.C. and Rutherford, M.J., 1989, Experimental calibration of the aluminium in hornblende geobarometer with application to long valley caldera (California) Volcanic Rocks. Geology, 17, 837–841. https://doi.org/10.1130/0091-7613

Kennedy, A.K., Wotzlaw, J.F., Schaltegger, U., Crowley, J.L., and Schmitz, M., 2014, Eocene zircon reference material for microanalysis of U-Th-Pb isotopes and trace elements. The Canadian Mineralogist, 52, 409–421.

Kozlu, H., 1997, Tectono-stratigraphic units of the Neogene basins (İskenderun, Misis-Andirin) and their tectonic evolution in the eastern Mediterranean region. Unpublished Ph.D. Thesis, Natural Science Institute, Çukurova University, Adana, Turkey, p. 189. (in Turkish with English abstract)

Leake, B.E., Woolley, A.R., Arps C.E.S., Birch, W.D., Gilbert, M.C., Grice, J.D., Hawthorne, F.C., Kato, A., Kisch, H.J., Krivovichev, V.G., Linthout, K., Laird, J., Mandarino, J.A., Maresch, W.V., Nickel, E.H., Rock, N.M.S., Schumacher, J.C., Smith, D.C., Stephenson, N.C.N., Ungaretti, L., Whittaker, E.J.W., and Youzhi, G., 1997, Nomenclature of amphiboles; report of the subcommittee on amphiboles of the Internal Mineralogical Association, Commission on New Minerals and Mineral Names. American Mineralogist, 82, 1019–1037.

Liu, Y., Gao, S., Hu, Z., Gao, C., Zong, K., and Wang, D., 2010, Continental and oceanic crust recycling-induced melt-peridotite interactions in the Trans-North China Orogen: U-Pb dating, Hf isotopes and trace elements in zircons from mantle xenoliths. Journal of Petrology, 51, 537–571. https://doi.org/10.1093/petrology/egp082

Locock, A.J., 2014, An Excel spreadsheet to classify chemical analyses of amphiboles following the IMA 2012 recommendations. Computers & Geosciences, 62, 1–11.

Ludwig, K.R., 2003, User's manual for Isoplot 3.00: a geochronological toolkit for Microsoft Excel. Special Publication, Berkeley Geochronology Center, Berkeley, USA, 74 p.

Ludwig, K.R., 2011, User's manual for Isoplot/Ex, v. 4.15: a geochronological toolkit for Microsoft Excel. Special Publication, Berkeley Geochronology Center, Berkeley, USA, 76 p.

Luhr, J.F., 1992, Slab-derived fluids and partial melting in subduction zones: insights from two contrasting Mexican volcanoes (Colima and Ceboruco). Journal of Volcanology and Geothermal Research, 54, 1–18.

McDermott, F. and Hawkesworth, C., 1991, Th, Pb, and Sr isotope variations in young island arc volcanics and oceanic sediments. Earth and Planetary Science Letters, 104, 1–15.

Middlemost, E.A.K., 1994, Naming materials in the magma igneous rock system. Earth-Science Reviews, 37, 215–224.

Mutch, E.J.F., Blundy, J.D., Tattitch, B.C., Cooper, F.J., and Brooker, R.A., 2016, An experimental study of amphibole stability in low-pressure granitic magmas and a revised Al-in-hornblende geobarometer. Contributions to Mineralogy and Petrology, 171, 1–27. https://doi.org/10.1007/s00410-016-1298-9

Nachit, H., Ibhi, A., Abia, E.H., and Ohoud, M.B., 2005, Discrimination between primary magmatic biotites, reequilibrated biotites and neoformed biotites. Comptes Rendus Géoscience, 337, 1415–1420. https://doi.org/10.1016/j.crte.2005.09.002

Nurlu, N., 2016, Geochemistry and tectonic signifiance of the tectonomagmatic units in the Helete (Kahramanmaraş) Region. Ph.D. Thesis, Çukurova University, Balcali-Adana, Turkey, 281 p.

Nurlu, N., 2020, Geochronological, geochemical and Sr-Nd-Pb isotope characteristics of the Meydan Ophiolite, SE Turkey: petrogenesis and implications for Mesozoic tectonic evolution. Geochemistry International, 58, 639–669. https://doi.org/10.1134/S0016702920060099

Nurlu, N., Parlak, O., Robertson, A.H.F., and Quadt, A.V., 2016, Implications of Late Cretaceous U-Pb zircon ages of granitic intrusions cutting ophiolitic and volcanogenic rocks for the assembly of the Tauride allochthon in SE Anatolia (Helete area, Kahramanmaraş Region, SE Turkey). International Journal of Earth Sciences, 105, 283–314. https://doi.org/10.1007/s00531-015-1211-1

Oberhansli, R., Candan, O., Bousquet, R., Rimmele, G., Okay, A., and Goff, J., 2010, Alpine high pressure evolution of the eastern Bitlis complex, SE Turkey. In: Sosson, M., Kaymakçı, N., Stephenson, R., Strarostenko, V., and Bergerat, F. (eds.), Sedimentary Basins, Tectonics from Black Sea and Caucasus to the Arabian Platform. Geological Society, London, Special Publications, 340, p. 461–483. https://doi.org/10.1144/SP340.20

Patiño Douce, A.E. and McCarthy, T.C., 1998, Melting of crustal rocks during continental collision and subduction. In: Hacker, B.R. and Liou, J.G. (eds.), When Continents Collide: Geodynamics and Geochemistry of Ultrahigh-Pressure Rocks. Petrology and Structural Geology, Springer, Dordrecht, Netherlands, 10, p. 27–55.

Paton, C., Hellstrom, J., Paul, B., Woodhead, J., and Hergt, J., 2011, Iolite: freeware for the visualization and processing of mass spectrometric data. Journal of Analytical Atomic Spectrometry, 26, 2508–2518. https://doi.org/10.1039/C1JA10172B

Pearce, J.A., 1982, Trace element characteristics of lavas from destructive plate boundaries. In Thorpe, R.S. (ed.), Andesites: Orogenic Andesites and Related Rocks. Wiley, London, UK, p. 525–548.

Pearce, J.A., 1983, Role of the subcontinental lithosphere in magma genesis at active continental margins. In: Hawkesworth, C.J. and Norry, M.J. (eds.), Continental Basalts and Mantle Xenoliths. Shiva Press, Nantwich, UK, p. 230–249.

Pearce, J.A., 2008, Geochemical fingerprinting of oceanic basalts with applications to ophiolite classification and the search for Archean oceanic crust. Lithos, 100, 14–48. https://doi.org/10.1016/j.lithos.2007.06.016

Pearce, J.A. and Stern, R.J., 2006, Origin of back-arc basin magmas: trace element and isotope perspectives. In: Christie, D.M., Fisher, C.R., Lee, S.-M., and Givens, S. (eds.), Back-Arc Spreading Systems: Geological, Biological, Chemical, and Physical Interactions. AGU Geophysical Monograph Series, American Geophysical Union, 166, p. 63–86. https://doi.org/10.1029/166GM06

Pearce, J.A., Stern, R.J., Bloomer, S.H., and Fryer, P., 2005, Geochemical mapping of the Mariana arc-basin system: implications for the nature and distribution of subduction components. Geochemistry, Geophysics, Geosystems, 6, 1–27. https://doi.org/10.1029/2004GC000895

Peccerillo, A. and Taylor, S.R., 1976, Geochemistry of Eocene calcalkaline volcanic rocks from the Kastamonu area, northern Turkey. Contributions to Mineralogy and Petrology, 58, 63–91.

Pitcher, W.S., 1987, Granites and yet more granites forty years on. Geologische Rundschau, 76, 51–79.

Plank, T. and Langmuir, C.H., 1998, The chemical composition of subducting sediment and its consequences for the crust and mantle. Chemical Geology, 145, 325–394.

Pourteau, A., Sudo, M., Candan, O., Lanari, P., Vidal, O., and Oberhansli, R., 2013, NeoTethys closure history of Anatolia: insight from $^{40}Ar$-$^{39}Ar$ geochronology and P-T estimation in high-pressure metasediments. Journal of Metamorphic Geology, 31, 585–606. https://doi.org/10.1111/jmg.12034

Reagan, M.K., Ishizuka, O., Stern, R.J., Kelley, K.A., Ohara, Y., Blichert-Toft, J., Bloomer, S.H., Cash, J., Fryer, P., Hanan, B.B., Hickey-Vargas, R., Ishii, T., Kimura, J.I., Peate, D.W., Rowe, M.C., and Woods, M., 2010, Fore-arc basalts and subduction initiation in the Izu-Bonin-Mariana system. Geochemistry, Geophysics, Geosystems, 11, 1–17. https://doi.org/10.1029/2009GC002871

Robertson, A.H.F., 2002, Overview of the genesis and emplacement of Mesozoic ophiolites in the Eastern Mediterranean Tethyan region. Lithos, 65, 1–67. https://doi.org/10.1016/S0024-4937(02)00160-3

Robertson, A.H.F., 2004, Development of concepts concerning the genesis and emplacement of Tethyan ophiolites in the Eastern Mediterranean and Oman regions. Earth-Science Reviews, 66, 331–387. https://doi.org/10.1016/j.earscirev.2004.01.005

Robertson, A.H.F., Clift, P.D., Degnan, P., and Jones, G., 1991, Palaeogeographicand palaeotectonic evolution of the Eastern Mediterranean Neotethys. Palaeogeography, Palaeoclimatology, Palaeoecology. 87, 289–344. https://doi.org/10.1016/0031-0182(91)90140-M

Robertson, A.H.F. and Dixon, J.E., 1984, Introduction: aspects of the geological evolution of the Eastern Mediterranean. In: Dixon, J.E. and Robertson, A.H.F. (eds.), The Geological Evolution of the Eastern Mediterranean. Geological Society, London, Special Publications, 17, p. 1–74. https://doi.org/10.1144/GSL.SP.1984.017.01.02

Robertson, A.H.F., Ustaömer, T., Parlak, O., Ünlügenç, U.C., Taslı, K., and Inan, N., 2006, The Berit transect of the Tauride thrust belt, S Turkey: Late Cretaceous–Early Cenozoic accretionary/collisional processes related to closure of the southern Neotethys. Journal of Asian Earth Sciences, 27, 108–145. https://doi.org/10.1016/j.jseaes.2005.02.004

Rollinson, H., 1993, Using Geochemical Data: Evaluation, Presentation, Interpretation. Longman, Harlow, UK, 352 p.

Rubatto, D., 2002, Zircon trace element geochemistry: partitioning with garnet and the link between U-Pb ages and metamorphism. Chemical Geology, 184, 123–138. https://doi.org/10.1016/S0009-2541(01)00355-2

Schmidt, M.W., 1992, Amphibole composition in tonalite as a function of pressure: an experimental calibration of the Al-in-hornblende

barometer. Contributions to Mineralogy and Petrology, 110, 304–310. https://doi.org/10.1007/BF00310745

Şengör, A.M.C. and Yılmaz, Y., 1981, Tethyan evolution of Turkey: a plate tectonic approach. Tectonophysics, 75, 181–241.

Şengör, A.M.C., White, G., and Dewey, J.F., 1979, Tectonic evolution of the Bitlis suture, southeastern Turkey: implications for the tectonics of the Eastern Mediterranean. Rapports et procès-verbaux des réunions Commission internationale pour l'exploration scientifique de la Mer Méditerranée, 25/26, 95–97.

Seyitoğlu, G., Esat, K., and Kaypak, B., 2017, The neotectonics of southeast Turkey, northern Syria, and Iraq: the internal structure of the Southeast Anatolian Wedge and its relationship with recent earthquakes. Turkish Journal of Earth Sciences, 26, 105–126. https://doi.org/10.3906/yer-1605-21

Shervais, J.W., 1982, Ti-V plots and the petrogenesis of modern and ophiolitic lavas. Earth and Planetary Science Letters, 59, 101–118.

Sláma, J., Košler, J., Condon, D.J., Crowley, J.L., Gerdes, A., Hanchar, J.M., and Whitehouse, M.J., 2008, Plešovice zircon – a new natural reference material for U-Pb and Hf isotopic microanalysis. Chemical Geology, 249, 1–35. https://doi.org/10.1016/j.chemgeo.2007.11.005

Spear, J.A., 1981, An experimental study of hornblende stability and compositional variability in amphibolite. American Journal of Science, 281, 697–734.

Spear, J.A., 1984, Micas in igneous rocks. In: Bailey, S.W. (ed.), Reviews in Mineralogy. Mineralogical Society of America, Washington DC, USA, 13, p. 299–356. https://doi.org/10.1515/9781501508820-013

Stampfli, G.M., 2001, Tethyan Oceans. In: Bozkurt, E., Winchester, J.A., and Piper, D.A. (eds.), Tectonics and Magmatism in Turkey and the Surrounding Area. Geological Society, London, Special Publications, 173, p. 1–23. https://doi.org/10.1144/GSL.SP.2000.173.01.01

Sun, S.S. and McDonough, W.F., 1989, Chemical and isotopic systematics of oceanic basalts: implications for mantle composition and processes. In: Saunders, A.D. and Norry, M.J. (eds.), Magmatism in the Ocean Basins. Geological Society, London, Special Publications, 42, p. 313–345. https://doi.org/10.1144/GSL.SP.1989.042.01.19

Teipel, U., Eichhorn, R., Loth, G., Rohrmüller, J., Höll, R., and Kennedy, A., 2004, U-Pb SHRIMP and Nd isotopic data from the western Bohemian Massif (Bayerischer Wald, Germany): implications for upper Vendian and lower Ordovician magmatism. International Journal of Earth Sciences, 93, 782–801. https://doi.org/10.1007/s00531-004-0419-2

Ural, M., Sayit, K., Koralay, O.E., and Goncuoglu, M.C., 2021, Geochemistry and zircon U-Pb dates of felsic-intermediate members of the Late Cretaceous Yüksekova Arc Basin: constraints on the evolution of the Bitlis-Zagros Branch of Neotethys (Elazığ, E Turkey). Acta Geologica Sinica (English Edition), 95, 1199–1216. https://doi.org/10.1111/1755-6724.14694

Usta, D., Ateş, Ş., Beyazpirinç, M., Kanar, F., Yıldız, H., Uçar, L., and Örtlek, A.T., 2015, New data on the stratigraphy of the central and northern Amonous Mountains (Osmaniye-Gaziantep-K.Maras). TAPG Bulletin, 27, 57–98.

van Hinsbergen, D.J.J., Torsvik, T.H., Schmid, S.M., Majenc, L.C., Maffione Visser, M.R., Gürer, D., and Spakman, W., 2020, Orogenic architecture of the Mediterranean region and Kinematic reconstruction of since the Triassic. Gondwana Research, 81, 79–229. https://doi.org/10.1016/j.gr.2019.07.009

Wang, T., Wang, Z., Yana, Z., Ma, Z., He, S., Fua, C., and Wang, D., 2016, Geochronological and geochemical evidence of amphibolite from the Hualong Group, northwest China: implication for the early Paleozoic accretionary tectonics of the Central Qilian belt. Lithos, 248–251, 12–21.

Wiedenbeck, M., Alle, P., Corfu, F., Griffin, W., Meier, M., Oberli, F., Quadt, A.V., Roddick, J., and Spiegel, W., 1995, Three natural zircon standards for U-Th-Pb, Lu-Hf, trace element and REE analyses. Geostandards Newsletter, 19, 1–23. https://doi.org/10.1111/j.1751-908X.1995.tb00147.x

Willbold, M. and Stracke, A., 2006, Trace element composition of mantle endmembers: implications for recycling of oceanic and upper and lower continental crust. Geochemistry, Geophysics, Geosystems, 7, 1–18. https://doi.org/10.1029/2005GC001005

Wilson, M., 1989, Igneous Petrogenesis: A Global Tectonic Approach. Unwin Hyman, London, UK, 466 p.

Winchester, J.A. and Floyd, P.A., 1977, Geochemical discrimination of different magma series and their differentiation products using immobile elements. Chemical Geology, 20, 325–343.

Yalçın, N., 1980, Lithological characteristics of the Amanos mountain range and its significance on the tectonic evolution of the Southeast Turkey. Bulletin of the Geological Society of Turkey, 23, 21–30.

Yamamoto, T., 2007, A rhyolite to dacite sequence of volcanism directly from the heated lower crust: Late Pleistocene to Holocene Numazawa Volcano, NE Japan. Journal of Volcanology and Geothermal Research, 167, 119–133. https://doi.org/10.1016/j.jvolgeores.2007.05.011

Yılmaz, Y., 1993, New evidence and model evolution of the southeast Anatolian orogen. Geological Society of America Bulletin, 105, 251–271.

Yılmaz, Y., 2018, Southeast Anatolian Orogenic Belt revisited (geology and evolution). Canadian Journal of Earth Sciences, 56, 1163–1180. https://doi.org/10.1139/cjes-2018-0170

Yılmaz, Y., 2021, Geological correlation between northern Cyprus and southern Anatolia. Canadian Journal of Earth Sciences, 58, 640–657. https://doi.org/10.1139/cjes-2020-0129

Yılmaz, Y. and Gürer, Ö.F., 1996, The geology and evolution of the Misis-Andirin Belt, around Andirin (Kahramanmaraş). Turkish Journal of Earth Sciences, 5, 39–55. (In Turkish with English abstract)

Yılmaz, Y., Yiğitbas, E., and Genç, S., 1993, Ophiolitic and metamorphic assemblages of Southeast Anatolia and their significance in the geological evolution of the orogenic belt. Tectonics, 12, 1280–1297.

**Publisher's Note** Springer Nature remains neutral with regard to jurisdictional claims in published maps and institutional affiliations.